MODELING THE EFFECTIVE MECHANICAL PROPERTIES OF ''FUZZY FIBER'' COMPOSITES

S.A. Lurie[a,b,i], D.B. Volkov-Bogorodskiy[a], O. Menshykov[h], Y.O. Solyaev[a,i], E.C. Aifantis[c,d,e,g,f]

[a]Lomonosov Moscow State University
[b]Institute for Problems in Mechanics of RAS, Moscow, Russia
[c]Aristotle University of Thessaloniki, Thessaloniki 54124, Greece
[d]Michigan Technological University, Houghton, MI 49931, United States
[e]BUCEA, Beijing 100044, China
[g]ITMO University, St. Petersburg 197101, Russia
[f]Togliatti State University, Togliatti 445020, Russia
[h]School of Engineering, University of Aberdeen, AB24 3UE, Scotland, UK
[i]Dorodnicyn Computing Center of FRC CSC RAS, Moscow, Russia

Abstract

We employ a variant of generalized Eshelby's homogenization method to deduce effective properties of multilayered nanostructured fiber composites where one layer is highly heterogeneous with respect to its mechanical response strain gradients. We focus on carbon (C) fibers coated by carbon nanotubes (CNT) embedded in polymeric matrix with the aid of CNT "blistered" interphase layer developed between the coating and the matrix during processing and/or use.

Each of the three phases is treated for simplicity by classical elasticity, while the interphase layer around the coated fibers ("fuzzy fibers") to provide adhesion, and is treated by the simple gradient elasticity (GradELa) model.

The novelty of the work lies on the fact of treating the CNT "fuzzy" layer by the GradEla model, that consequently allows to consider the extra gradient coefficient or internal length (characterizing this model) in relation to other constitutive and geometric parameters of the composite to optimize its overall mechanical properties and functionality. The method is general and can apply to treat other types of "fuzzy fiber" composites.

Key words: fiber reinforced polymer composites, carbon nanotubes, fuzzy fibers, generalized self-consistent (GSC) method, effective mechanical properties

1. Introduction

In aerospace industry, fiber reinforced plastic (FRP) composite material can be tailored to produce very strong and stiff lightweight structures. However, the unique properties of fiber composites are often restricted by the poor mechanical properties of the fiber-matrix interface.

To improve the quality of the interface between fiber and matrix a variety of techniques may be applied, with the most approach being to introduce another material or an interphase

layer between fiber and matrix [1-4]. In [1] zinc oxide nanowires (ZnO NW) were radially coated on the surface of IM7 carbon fibers, while various types of coatings were used in [2] to enhance the interaction between fibers and matrix. Here, in particular, a nanostructured layer consisted of a forest of carbon nanotubes (CNTs) grown on coated carbon fibers is considered. This results to a bristled of "fuzzy" interface phase which improves the interfacial adhesion properties, and increases the fiber's surface area for more effective load transfer between fiber and matrix. The situation is analogous to "whiskered fibers" embedded to an epoxy matrix, resulting [3] in increase of the shear strength of the composite by 200–400% (depending of the properties of the carbon fibers and epoxy matrix). Thus the practical implementation of these ideas led to fabrication of a new class of modern multifunctional composites. According to the review of [4], multifunctional composites are now being designed for simultaneous enhancement of strength, stiffness, toughness, fatigue, damping, and thermal conductivity.

The influence on fracture toughness of multi-walled carbon-nanotubes grown on both sides of the carbon-fiber fabric lamina and on the surface of the woven carbon-fiber fabric were studied in [5]. In addition, the presence of single walled nanotubes in the polymer matrix leads to an increase in the modulus of elasticity of CNT/polymer composites. In [6] the resulting enhanced effect is estimated using the Mori Tanaka method. It was shown that the multi-walled CNT layer has the potential for sensing and accommodating the internal matrix damage. In [7] it was shown that CNTs grown on carbon fibers enhance the in-plane and out-of-plane properties of fiber reinforced polymer composites. In particular, it was concluded that the on-axis tensile strength and ductility of the hybrid polymers were improved by 11% and 35%, respectively, due to the presence CNTs. The positive effect of CNT waviness on the effective coefficient of thermal expansion of a novel continuous fuzzy fiber reinforced composite was established in [8]. Using 3D multiscale computational models the authors of [9] demonstrated the potential benefits of advanced carbon/glass hybrid reinforced composites with secondary CNT reinforcement for wind energy applications. It is shown in [10] that the presence of multiwalled carbon nanotubes (MWCNTs) on the surface of aramid fibers leads to an increase of the interfacial of aramid shear strength due to increased fiber surface roughness. A comprehensive experimental investigation was conducted in [11] to elucidate the viscoplastic behavior of hybrid polymer matrix composites based on carbon fiber/CNT reinforcement. It was shown that a patterned growth of the CNTs on the carbon fibers lead to improvements on creep deformation and stress relaxation.

A recent method employed to improve the shear performance of a fiber reinforced composite is to grow a nanoforest from CNTs directly on top of the surface of carbon fibers. Such a fiber system, commonly known as "fuzzy fiber" [12], exhibits increased compressive strength in the redial direction along which the CNTs are aligned. Significant fracture toughness

enhancement can also be obtained when the CNTs are aligned such that to reinforce crack interfaces [13]. In a recent review [14] the effect of coating through radial aligned carbon nanotubes on carbon fibers ("fuzzy fibers") on the mechanical properties was analyzed. It was demonstrated that the fuzzy fibers result to improved transverse properties as compared to uncoated composites. Even small additions of CNTs have a very strong effect on these properties. Thus, fuzzy fiber composite material seems to be very promising material.

Further experimental work [15] revealed that the length and density of CNTs grown on top of the surface of carbon fiber are critical factory controlling the enhanced functional properties of CNT-coated carbon/polyester composite materials. Moreover, improved chemo mechanical stability and prevention of strength loss can be established by the "hierarchy" of nanostructures in carbon fiber composites [16].

Presently, there are several micromechanics models proposed by various authors that may be used to determine the effective mechanical properties of "bristled" of "fuzzy" fiber composite materials. In [17, 18] such composites consisting of four layers (namely, a base fiber, a fiber-coating layer, a bristled interphase layer, and the matrix material) were studied. This four-component structural model, based on a periodic unit cell, was used to extract the overall effective properties of composites with whiskered fibers by using a two-step homogenization procedure. The first step involves the homogenization of a bristled interphase layer by using the rule of mixtures. In the second step of homogenization procedure, the properties of all phases in the four-component structural model are averaged.

Other authors proposed analytical models to predict the effective elastic properties of bristled fiber composites based on generalized self-consistent Eshelby method [19], or the Mori–Tanaka method [20], to derive the effective properties for three-phase fuzzy fiber composites. The effect of diameter of CNTs, as well as the effect of an interphase between CNT and matrix, on the overall properties of fuzzy fiber composites were investigated, but the effect of density (quantity) of CNT's was not considered. The results obtained by both methods were in good agreement. It was shown that the presence of CNTs significantly increases the effective transverse elastic constants, while the effective in-plane elastic constant is not affected. At the same time, these constants increased marginally with the increase in CNTs' diameter, and the role of an interphase was found to be insignificant.

In [12] (and related references quoted therein) a combined approach based on a numerical procedure of asymptotic homogenization for the assemblage of the CNTs forest and generalized self-consistent method was employed to fully describe the effective properties of a three-phase fuzzy fiber composites. The effective properties of the CNT interphase layer were modelled by

using the numerical implementation of asymptotic expansion homogenization method (AEH) for periodic unit cells.

The analytical and numerical results revealed that the transverse and shear properties of fuzzy fiber composites are strongly influenced by the presence of CNTs, while the effect on the axial Young's modulus is nearly marginal. The effects of length and volume fraction of CNTs were also examined, and it was found that both parameters significantly affect the properties of fuzzy fiber composite materials.

In the present paper we depart from previous works by adopting the analytical approach based on the generalized self-consistent method [13] and assuming that the interphase fuzzy layer is described by the GradEla model, used earlier to derive effective properties of "gradient" composites [21]. A recent review on the GradEla model along with the applications including elimination of elastic singularities from dislocation lines and crack tips can be found in [22] along with an extensive number of references on the topic. Application of the generalized self-consistent Eshelby method allows to take into account variations of the "interphase layer" properties associated with changes in the density of nanofibers across the radial direction in the aligned CNT-forest. Moreover, application of the gradient model for interphase layer allows to compute the effective properties of the whole composite, which now depend, among other things, on an extra gradient or internal length parameter, thus providing another source for the appearance of size effects. Such a combination of the Eshelby methodology with Aifantis GradEla model was outlined in [21] and more recently utilized [23-25] to model locally-functional gradient properties and multilayered spherical inclusions. The properties of the fundamental solutions of the GradEla model (see references listed in [22]) are also taken into account. General solutions in each sub-layer of the fibrous system are constructed using the general Papkovich-Neuber representation via potentials of the Laplace and Helmholtz type, along with the radial multipliers method [25, 26].

Another homogenization method for plastically deforming composites incorporating both gradient and surface energy effects has been proposed in [27]. This method may be applied to the present problem, a task to be considered in the future.

2. On gradient theories of elasticity

Let us consider the gradient theory of elasticity from the point of the potential energy. The potential energy of deformations E for the center-symmetric materials (expressed in terms of distortion gradients) has the following form [21, 22, 28]:

$$E = \frac{1}{2}\int_G [C_{ijkl} R_{i,j} R_{k,l} + C_{ijklmn} R_{i,jk} R_{l,mn}] dG , \tag{1}$$

where $C_{ijkl} = \lambda\delta_{ij}\delta_{kl} + \mu(\delta_{ik}\delta_{jl} + \delta_{il}\delta_{jk})$, with δ_{ij} being the Kronecker delta, (λ, μ) the Lamé coefficients, C_{ijklmn} a six-order tensor of gradient elasticity moduli for isotropic materials, G the volume of the gradient elastic body (we use the symbol G instead of V in order to conform with the notation of [21]). It is noted that Eq. (1) is a slight generalization of so-called GradEla model [22] where instead of strains (the symmetric part of $R_{i,j}$), we use the distortion or displacement gradient tensor ($R_{i,j}$).

The components of the Cauchy-like stress tensor σ_{ij} and the double stress tensor μ_{ijk} are defined by:

$$\sigma_{ij} = \partial E / \partial R_{i,j} = C_{ijkl} R_{k,l}, \quad \mu_{ijk} = \partial E / \partial R_{i,jk} = C_{ijklmn} R_{l,mn}. \tag{2}$$

The following symmetry conditions are satisfied for the classical and gradient moduli in Eqs. (1) and (2)

$$C_{ijkl} = C_{klij}, \quad C_{ijklmn} = C_{lmnijk}. \tag{3}$$

Thus the gradient theory of elasticity, in which the gradient part of the potential energy is determined by the distortion tensor, we will call the gradient elasticity of distortion. In the case that the potential energy is expressed in terms of the symmetric strain tensor and its special derivatives, the additional condition of symmetry $C_{ijklmn} = C_{jiklmn}$ must be introduced.

In [26] it was shown that Eq. (3) must be written only for the symmetric part of the double stress tensor with respect two last indexes. Consequently, for the gradient elasticity the boundary value problem should be formulated only for the symmetric part of the double stress tensor $\mu_{ijk} = \mu_{ikj}$. Then, the tensor of gradient modulus must satisfy the potential conditions $C_{ijkl} = C_{klij}$, $C_{ijklmn} = C_{lmnijk}$ and also the necessary symmetry conditions of the order of differentiation, $C_{ijkl} = C_{ijlk}$, $C_{ijklmn} = C_{ijklnm}$.

Let us consider the variational formulation of the gradient elasticity of distortion

$$\begin{aligned} &\delta L = 0, \ L = U - A, \ A = \int_G f_i R_i dG + \iint_{\partial G} (t_i R_i + q_i R_{i,j} n_j) d(\partial G), \\ &\delta L = \int_G (\sigma_{ij,j} - m_{ijk,kj} + f_i)\delta R_i dG + \\ &+ \iint_{\partial G} \{[t_i - (\sigma_{ij} - m_{ijk,k})n_j]\delta R_i - m_{ijk} n_k \delta R_{i,j}\} d(\partial G) = 0, \end{aligned} \tag{4}$$

where volume integrals are taken over the domain G occupied by the body before the deformation, the surface integrals are taken over the closed smooth boundary surface ∂G of the domain G, A is the work done by external body force f_i and Cauchy-like traction t_i, R_i is the

displacement vector, $R_{i,j} = \partial R_i / \partial x_j$, $R_{i,jk} = \partial^2 R_i / \partial x_j \partial x_k$, and n_i are the components of the outward unit normal vector on ∂G (further we assume that $q_i = 0$).

The second term $m_{ijk} n_k \delta R_{i,j}$ in the surface integral (4) is the sum of nine terms. Three of them contain the multipliers of the variation of the normal derivatives of displacements, and the other six contain variations of the tangential derivatives of displacements. Since the tangential derivatives of displacements and displacements are not entirely independent, the appropriate terms are integrated by parts. Usually this is done in the following manner:

$$\begin{aligned}
&\iint_{\partial G} \{[f_i - (\sigma_{ij} - m_{ijk,k}) n_j] \delta R_i - m_{ijk} n_k \delta R_{i,j}\} d(\partial G) = \\
&= \iint_{\partial G} \{[f_i - (\sigma_{ij} - m_{ijk,k}) n_j + (m_{ijk} n_k)_{,p} (\delta_{pj} - n_p n_j)] \delta R_i - m_{ijk} n_j n_k \delta (R_{i,p} n_p)\} d(\partial G) - \\
&- \sum \int\!\!\!\!\!\!\int m_{ijk} \nu_j n_k \delta R_i ds = 0.
\end{aligned} \tag{5}$$

The traditional approach, in general, leads to the "modification" of the classical static boundary conditions by introducing in Eq. (5) a non-classical term $(m_{ijk} n_k)_{,p} (\delta_{pj} - n_p n_j)$, and to the appearance of additional requirements for the continuity of the displacement vector δR_i and the vector of the “meniscus” forces $m_{ijk} \nu_j n_k$ when passing to the surface.

There is the unique simple form of gradient theory of elasticity (the GradEla model) where the tensor of gradient moduli of the sixth order has the special form:

$$C_{ijkmnl} = (l^2 / \mu) C_{rkij} C_{rlmn} . \tag{6}$$

Here l denotes the internal length parameter representing the spatial arrangement of the underlying micro/nano structure.

For the simplified gradient model with the tensor of gradient elastic moduli given by Eq. (6), the static boundary condition for the variation of the displacements of the shape δR_i in the surface integral is written with respect the “classical” stresses $\sigma_{ij} - m_{ijk,k}$ only. As a result, the variational form $m_{ijk} n_j n_k \delta (R_{i,p} n_p)$ for the moment boundary conditions given by Eq. (5) is represented as a linear variational form with respect to the variations of three linearly independent combinations of normal and tangential derivatives of the displacement.

The tensor of the “classical” stresses (corresponding to the real Cauchy strain of classical elasticity) has the form:

$$s_{ij} = (\sigma_{ij} - m_{ijk,k}) = C_{ijmn} R_{m,n} - (l^2 / \mu) C_{rlmn} R_{m,nlk} = C_{ijmn} U_{m,n} = \sigma_{ij}(\mathbf{U}) , \tag{7}$$

where $\sigma_{ij}(\boldsymbol{U})$ is the stress operator under vector

$$U_i = R_i - (l^2 / \mu) C_{icab} R_{a,bc} . \tag{8}$$

As a result, the potential energy has the form:

$$E = \frac{1}{2}\int_G \left[C_{ijnm}\, R_n,_m\, R_i,_j + (l^2/\mu) C_{rkij} C_{rlmn} R_i,_{jk}\, R_n,_{lm}\right] dG = \\ = \frac{1}{2}\int_G \left[C_{ijnm}\, R_n,_m\, R_i,_j + C\, u_i\, u_i\right] dG, \tag{9))}$$

where $u_i = -(l^2/\mu) C_{icab} R_{a,bc}$, or $u_i = -(1/C) L_{ij}(R_j)$, $C^{-1} = l^2/\mu$. The quantity u_i is the vector of the "cohesion" displacements, which satisfies to the Helmholtz equation $(L_{ij} - C\delta_{ij})(u_i) = 0$, where L_{ij} is the Lamé operator of the classical theory of elasticity (see, for example, [22] references listed therein on Ru-Aifantis theorem), and $U_i = R_i - u_i$ is the vector of "classical" displacements.

Using Eq. (9), the variational equation may be rewritten in the following form:

$$\delta L = \int_G [(s_{ij,j} + f_i)\delta R_i dG + \iint_{\partial G} (t_i - s_{ij} n_j)\, \delta R_i\, d(\partial G) - \\ - \iint_{\partial G} (C^{-1})(C_{rlmn} R_{m,nl}) \delta (C_{rkij} R_{i,j} n_k) d(\partial G). \tag{10}$$

Thus, in view of Eq. (10), the equilibrium equations and the static boundary conditions are formulated with respect to the "classical" stress tensor $s_{ij} = C_{ijmn} U_{m,n} = \sigma_{ij}(\boldsymbol{U})$, and all moment boundary conditions are formulated for the generalized vector of moments $(C^{-1})(C_{rlmn} R_{m,nl})$, signifying the work of the vector of generalized displacements $(C_{skij} R_{i,j}) n_k$, $(R_i = U_i - u_i)$ on the surface of the body.

In applications it is may be convenient to write the static boundary conditions in terms of "cohesion" u_i and "classical" U_i displacement fields

$$\delta L = \int_G [(\sigma_{ij,j}(\boldsymbol{U}) + f_i)\delta R_i dG + \\ + \iint_{\partial G} [t_i - \sigma_{ij}(\boldsymbol{U}) n_j - (T_{ij}(\boldsymbol{u}))_j + (T_i(\boldsymbol{u}))_k n_k]\, \delta R_i\, d(\partial G) - \\ - \iint_{\partial G} T_i(\boldsymbol{u}) \delta [(R_{i,k}) n_k] d(\partial G).$$

where $C_{rkij} n_k n_j u_r = T_i(\boldsymbol{u}), \quad T_{ij}(\boldsymbol{u}) = C_{rkij} n_k u_r$.

It can be verified that among all models with potential energy given by Eq. (9) there is a unique model for the gradient stiffness matrix C_{ijklmn} for which the potentiality conditions and necessary symmetry conditions are fulfilled $C_{ijklmn} = C_{ijklnm}$ [24]:

$$C_{ijklmn} = \frac{\mu}{C}\left[\mu\,\delta_{jk}\delta_{il} + \frac{\mu+\lambda}{2}\left(\delta_{ik}\delta_{jl} + \delta_{ij}\delta_{kl}\right)\right]\delta_{mn} +$$
$$+\frac{\mu+\lambda}{2C}\left\{\left[\mu\,\delta_{jk}\delta_{im} + \frac{\mu+\lambda}{2}\left(\delta_{ik}\delta_{jm} + \delta_{ij}\delta_{km}\right)\right]\delta_{ln} + \left[\mu\,\delta_{jk}\delta_{in} + \frac{\mu+\lambda}{2}\left(\delta_{ik}\delta_{jn} + \delta_{ij}\delta_{kn}\right)\right]\delta_{lm}\right\}. \quad (11)$$

The choice of the matrix C_{ijklmn} in the form of Eq. (11) corresponds to an asymmetric tensor of the moment stresses μ_{ijk}; so the model defined by Eqs.(1) – (3), (6) – (9) and (11) corresponds to the gradient elasticity of distortions, where $C_{ijklmn} \neq C_{jiklmn}$, and the third-rank moments tensor satisfies the symmetry condition $\mu_{ijk} = \mu_{ikj}$ for the last two indices.

The gradient model defined by Eqs. (1) – (3), (6) – (9) and (11) will be used to describe the properties of the CNTs interphase layer and to estimate the effective properties of the fibrous composite. At the same time, the variability of the properties of the interphase layer with respect to the radial coordinate will be modeled according to the localization of the gradient solution [29].

3. Contact boundary conditions for the Eshelby problem of the CNT fuzzy fiber composite

We study the effective mechanical characteristics of a fiber composite material reinforced by straight fibers with CNT fuzzy layers by employing the self-consistent Eshelby's model of four cylindrical bodies. The density of the CNT nanotubes varies near the surface of the base fibers and the effective characteristics of the interfacial "fuzzy" layer of whiskers depend on the distance r from the surface of the base fibers. To take into account the variability of CNT interphase layer we propose to use the aforementioned gradient theory. We believe that the gradient solution is particularly suitable for describing the functional graded material properties, such as exponential changes near zones of the contacted phases.

Thus, we consider an analytical method for constructing explicit solutions of the generalized Eshelby problem, which can be called the method of radial coefficients. The solution of the general problem for the displacements is constructed with the aid of a generalized Papkovich-Neuber representation. This representation contains, in particular, the classical representation of the theory of elasticity for vanishing cohesive field. Initially, we consider a more traditional configuration made up from three cylindrical bodies, and determine the variable characteristics of the CNT interphase layer itself. Then, in order to define the effective properties of the "fuzzy" fiber composite as whole and to take into consideration the functional gradient properties of the CNT interphase layers, a more general configuration made up by four cylindrical bodies with a gradient model for the interphase layer is used.

The generalized Eshelby problem is solved for the cylindrical fragment that is presented in Fig. 1. It is assumed that the cylinders are arranged along the axis z. The intermediate phase

G_L is described by the gradient elasticity model. The remaining phases are described by the Lamé equations of classical elasticity. The problem is to consider the multilayered structure (see Fig. 1) and to obtain a solution of the generalized Eshelby problem for an isolated complex inclusion in a matrix under the uniform deformation at infinity.

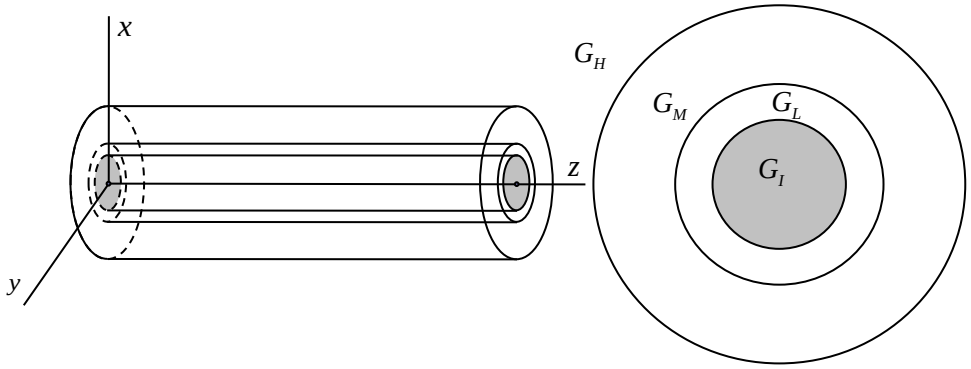

Fig.1. A four-body configuration for a fiber-reinforced composite with a fuzzy layer

This gradient theory of elasticity formulation can be written using the following representation (see [24]) of the displacements through the auxiliary potentials $\boldsymbol{f}_0$, ϕ_0 and $\boldsymbol{f}$, $\boldsymbol{f}^*$ satisfying the Laplace and Helmholtz equations:

$$\boldsymbol{R}(P) = \frac{\boldsymbol{f}_0 - \boldsymbol{f}}{\mu} + \nabla\left[\frac{\phi_0 - \boldsymbol{r}\,\boldsymbol{f}_0}{4\mu\,(1-\nu)} - \mathrm{div}\left(\frac{\boldsymbol{f}^* - \boldsymbol{f}}{C}\right)\right], \tag{12}$$

$$\nabla^2 \boldsymbol{f}_0 = \nabla^2 \phi_0 = 0\,, \quad \nabla^2 \boldsymbol{f} - \frac{C}{\mu}\boldsymbol{f} = 0\,, \quad \nabla^2 \boldsymbol{f}^* - \frac{C}{k}\boldsymbol{f}^* = 0\,, \quad k = 2\mu + \lambda\,. \tag{13}$$

As before, μ is the shear modulus, ν is thePoisson ratio, λ is the Lamé cefficient and C is a scale parameter, signifying the changing of characteristics in the whiskers “fuzzy” layer.

The representation embodied in Eqs. (12), (13) also provides a solution of the classical elasticity theory in the case when $C \to \infty$ (potentials $\boldsymbol{f}$ and $\boldsymbol{f}^*$ are zero). The form of the representation given by Eq. (12) allows us to divide the general vector of displacements $\boldsymbol{R}$ into the vector of classical displacements $\boldsymbol{U}$ and vector of cohesion displacements $\boldsymbol{u}$:

$$\boldsymbol{R} = \boldsymbol{U} - \boldsymbol{u}\,, \quad \boldsymbol{U}(P) = \frac{\boldsymbol{f}_0}{\mu} + \frac{\nabla(\phi_0 - \boldsymbol{r}\,\boldsymbol{f}_0)}{4\mu\,(1-\nu)}\,, \quad \boldsymbol{u}(P) = \frac{\boldsymbol{f}}{\mu} + \frac{\nabla\,\mathrm{div}(\boldsymbol{f}^* - \boldsymbol{f})}{C}\,. \tag{14}$$

Here $\boldsymbol{u}(P)$ is an additional field of exponential type, determined by the Helmholtz equations given by Eq. (13). This field introduces an additional exponential variability to the field of classical displacements $\boldsymbol{U}(P)$ associated with the variable characteristics of the layer. We assume that the cohesion field vanishes in the regions G_I, G_M and G_H.

The method presented in this section is valid for an arbitrary number of layers and for an arbitrary combination of gradient and classical interphase regions. Contact conditions on the interface boundaries include another set of different equations, depending on the nature of the contact between two gradient layers, or between a gradient and a classical layer, or between two

classical layers. Correspondingly, the number of vector contact equations is four, three or two. In the case of contact of two regions, one of which is described in the framework of the classical elasticity and the other by the gradient elasticity, the contact conditions have the following form:

$$\left[\boldsymbol{R}\right]=\left[\boldsymbol{p}(\boldsymbol{U})-\hat{\boldsymbol{p}}(\boldsymbol{u})\right]=0\,,\quad \frac{\partial \boldsymbol{R}}{\partial n}=0\,,\quad \hat{\boldsymbol{p}}(\boldsymbol{u})=\frac{\partial (T_j\boldsymbol{u})}{\partial x_j}-\frac{\partial (T\boldsymbol{u})}{\partial n}\,,\ P\in\partial G_I\cup\partial G_M\,, \tag{15}$$

where the 3×3 matrices T_j and T are expressed in terms of the material characteristics and the components of the normal vector at the boundary are as follows:

$$T_j=\left\{-\mu\left(\delta_{kl}\,n_j+\delta_{jl}n_k\right)-\lambda\,\delta_{jk}n_l\right\},\qquad T=T_j\,n_j=\left\{-\mu\,\delta_{kl}-(\mu+\lambda)\,n_k n_l\right\},$$

where $\boldsymbol{p}(\boldsymbol{U})=\left\{\sigma_{ij}(\boldsymbol{U})n_j\right\}$ are the surface stresses defined on the classical displacement field, with n_i being as usual the normal unit vector, and $\left[\cdot\right]$ denoting the jump of the respective quantity at the interface boundary.

In the most general case of contact of two gradient layers, the boundary conditions can be obtained directly from the variation of Eq. (9). On the other hand, it is useful to represent the boundary conditions in terms of classical and cohesive displacement fields. To do that let us consider the bilinear form corresponding to the energy functional given by Eq. (9) and rewrite this equation using integration by parts:

$$E(\boldsymbol{R},\boldsymbol{R}')=\int\limits_G\left[2\mu\,\varepsilon_{ij}\,\varepsilon'_{ij}+\lambda\,\theta\,\theta'+\frac{(L_{ij}R_j)(L_{ij}R'_j)}{C}\right]dG=\int\limits_{\partial G}p_i(\boldsymbol{R}')R_i\,d(\partial G)-\int\limits_G(L_{ij}R'_j)\,U_i\,dG\,,$$

where $U_i=R_i-L_{ij}R_j/C$, $L_{ij}=(\lambda+\mu)\partial_i\,\partial_j+\delta_{ij}\,\mu\nabla^2$.

Next, we use integration by parts for the second terms in the last equation and take into account the expansion $\boldsymbol{R}=\boldsymbol{U}-\boldsymbol{u}$. As a result, we find the following equation:

$$E(\boldsymbol{R},\boldsymbol{R}')=\int\limits_G f_iR'_i dG+\int\limits_{\partial G}\left[p_i(\boldsymbol{U})R'_i-u_i\,p_i(\boldsymbol{R}')\right]d(\partial G)=\int\limits_G f_iR'_i dG+\int\limits_{\partial G}\left[\boldsymbol{p}(\boldsymbol{U})\boldsymbol{R}'+(T_j\boldsymbol{u})\frac{\partial \boldsymbol{R}'}{\partial x_j}\right]d(\partial G)=$$

$$=\int\limits_G f_iR'_i dG+\int\limits_{\partial G}\left[\boldsymbol{p}(\boldsymbol{U})-\frac{\partial (T_j\boldsymbol{u})}{\partial x_j}+\frac{\partial (T\boldsymbol{u})}{\partial n}\right]\boldsymbol{R}'d(\partial G)+\int\limits_{\partial G}(T\boldsymbol{u})\frac{\partial \boldsymbol{R}'}{\partial n}d(\partial G),\quad T=T_j n_j.$$

Thus, we obtained the integral Green's formula, along with the following boundary conditions (see also [25]):

$$\left[\boldsymbol{R}\right]=\left[\frac{\partial \boldsymbol{R}}{\partial n}\right]=0\,,\quad \left[T\boldsymbol{u}\right]=\left[\boldsymbol{p}(\boldsymbol{U})-\hat{\boldsymbol{p}}(\boldsymbol{u})\right]=0\,,\quad \hat{\boldsymbol{p}}(\boldsymbol{u})=\frac{\partial (T_j\boldsymbol{u})}{\partial x_j}-\frac{\partial (T\boldsymbol{u})}{\partial n}\,. \tag{16}$$

These equations represent the continuity condition for the general displacement together with their first-order spatial derivatives, and also the continuity of the surface and double stresses $T\boldsymbol{u}$ determined by the values of the cohesive field at the interface boundary. The additional condition $\partial \boldsymbol{R}/\partial n=0$ on the interface boundary of the "classical" domain follows from the integral

Green's formula under the additional assumption that the cohesion field vanishes in this domain. Note, that another possible condition for the interface boundary of the classical domain is $\boldsymbol{u}(P)=0$, but the condition of smooth joining of the respective layers $\partial \boldsymbol{R}/\partial n=0$ is more preferable.

Thus, it is required to construct a vector function $\boldsymbol{R}(P)$ in the form given by Eqs. (12) – (14) which satisfies the contact boundary conditions given by Eq. (15) with a linear asymptotic behavior at infinity corresponding to the homogeneous deformation state given by the displacements field $\boldsymbol{U}^{(H)}$:

$$\boldsymbol{R}(P)\to\boldsymbol{U}^{(H)},\quad \boldsymbol{U}^{(H)}=\left\{\varepsilon_{ij}^{(0)}x_j\right\},\quad P\to\infty.$$

For further convenience, the displacement $\boldsymbol{U}^{(H)}$ is defined by the Papkovich-Neuber representation with the harmonic polynomial of the first degree $\boldsymbol{f}^{(H)}$:

$$\boldsymbol{R}(P)\to\boldsymbol{U}^{(H)},\quad \boldsymbol{U}^{(H)}=\frac{\boldsymbol{f}^{(H)}}{\mu_H}-\frac{\nabla(\boldsymbol{r}\,\boldsymbol{f}^{(H)})}{4\mu_H(1-\nu_H)},\quad P=\{x,y,z\}\to\infty.$$

Here μ_H, ν_H, λ_H are the stiffness parameters for an isotropic homogeneous medium, corresponding to the effective characteristics of the Eshelby-Christensen model for the four cylindrical bodies.

4. The generalized Eshelby problem

The problem formulated above is defined in subdomains G_j for the solutions obtained with the aid of the auxiliary potentials in Eqs. (12)–(14) satisfying the homogeneous Helmholtz and Laplace equations. We must ensure that the asymptotic behavior of solutions for the equivalent homogenized medium (the phase G_H) has the form of an harmonic polynomial of the first degree. The solutions for the other phases (subdomains G_j) contain regular and singular potentials that are necessary for constructing these solutions in an explicit form with the necessary properties. These potentials can be represented as products of homogeneous harmonic polynomials of the first degree $\boldsymbol{f}^{(j)}(P)$ with the regular and singular radial multipliers h_1, $\hat{h}_1$, h_1^*, $\hat{h}_1^*$, $h_1^{(0)}$, $\hat{h}_1^{(0)}$, which are functions depending only on the radial coordinate in the cylindrical coordinate system:

$$h_1=\left(\frac{1}{r}\frac{d}{dr}\right)\left[I_0(\kappa r)\right],\quad \hat{h}_1=\left(\frac{1}{r}\frac{d}{dr}\right)\left[K_0(\kappa r)\right],\quad h_1^{(0)}=r^6,\quad \hat{h}_1^{(0)}=r^{-2}. \tag{17}$$

Here $\kappa=\sqrt{C/\mu}$ is the scale internal length parameter entering the Helmholtz equation and $I_0(z)$ is the modified Bessel function of zero order; $K_0(z)$ is the zero order MacDonald function (this is the fundamental solution of the Helmholtz equation on the plane); h_1^* and $\hat{h}_1^*$ are

determined by the same formulas given by Eq. (18), but with a different scale parameter $\kappa^* = \sqrt{C/k}$, $k = 2\mu + \lambda$. Note that the functions $\left(h_1,\ h_1^*,\ h_1^{(0)}\right)$ define the regular potentials and the functions with a superimposed hat $\left(\hat{h}_1,\ \hat{h}_1^*,\ \hat{h}_1^{(0)}\right)$ define the singular potentials.

In the method proposed, the potentials of the Papkovich-Neuber representation are determined via radial multipliers and basic harmonic polynomials of the first degree $\boldsymbol{f}^{(j)}$ in the regions G_j. The polynomials establish the connection of the local solutions with those of asymptotic behavior at infinity, and also allow to resolve the contact equations at the interface boundaries. This is possible, since radial multipliers have constant values on cylindrical surfaces. Linear relationships, that follow from the contact equations on the boundaries, are established between the coefficients of the basic polynomials and the corresponding ones at infinity. With each subdomain G_j a sufficient number of basic potentials is associated, and this number coincides with the number of contact equations on the interface boundaries.

To approximate the classical part $\boldsymbol{U}(P)$ of displacements, a system of four basic potentials is introduced in combination with the radial multipliers $h_1^{(0)} = r^6$ and $\hat{h}_1^{(0)} = r^{-2}$:

$$\boldsymbol{f}_1 = \boldsymbol{f}^{(j)}, \quad \boldsymbol{f}_2 = r^{-2}\boldsymbol{f}^{(j)}, \quad \boldsymbol{f}_3 = \nabla \operatorname{div}\left(r^{-2}\boldsymbol{f}^{(j)}\right), \quad \boldsymbol{f}_4 = r^6 \nabla \operatorname{div}\left(r^{-2}\boldsymbol{f}^{(j)}\right); \tag{18}$$

This system satisfies the Laplace equation (see also [24, 25]). Similarly, in order to approximate the cohesion field $\boldsymbol{u}(P)$ in all subdomains G_j – where the solution is determined by the gradient equations (for example, in the fuzzy layer G_L) – in addition to the potentials in Eq. (18), another system of four basic potentials in combination with the radial multipliers h_1, $\hat{h}_1$, h_1^* and $\hat{h}_1^*$ defined by Eq. (7) is introduced:

$$\boldsymbol{f}_5^* = h_1^*(r)\,\boldsymbol{f}^{(j)}, \quad \boldsymbol{f}_6^* = \hat{h}_1^*(r)\,\boldsymbol{f}^{(j)}, \quad \boldsymbol{f}_7 = h_1(r)\,\boldsymbol{f}^{(j)}, \quad \boldsymbol{f}_8 = \hat{h}_1(r)\,\boldsymbol{f}^{(j)}. \tag{19}$$

This system satisfies the Helmholtz equation (see also [24, 25]).

Substitution of the potentials of Eqs. (18), (19) into the generalized Papkovich-Neuber representation given by Eq. (12) and then use of the contact conditions given by Eqs. (15) and (16), transform the product of the radial factors and polynomial functions into a sum of several terms, which are linear combinations of some operators of basic harmonic polynomials with multipliers h_1, h_2, h_3:

$$\boldsymbol{F}(P) = h_1(r)\,\boldsymbol{f}^{(j)} + h_2(r)\,\boldsymbol{r}\ \operatorname{div}\boldsymbol{f}^{(j)} + h_3(r)\,\boldsymbol{r}(\boldsymbol{r}\,\boldsymbol{f}^{(j)}). \tag{20}$$

Here $\boldsymbol{F}(P)$ could be the displacement, its first order derivative, surface forces or moments accordingly to Eqs. (15), (16). Eq. (20) defines the form of the boundary function entering in the contact condition with coefficients h_1, h_2, h_3, which assume a constant value on the contact

surface. This consists of the basic polynomial $\boldsymbol{f}^{(j)}$, as well as the polynomial of planar expansion $\boldsymbol{r}$ div $\boldsymbol{f}^{(j)}$ and the biharmonic contribution $\boldsymbol{r}(\boldsymbol{r}\,\boldsymbol{f}^{(j)})$.

Below, a specific form of the expansion formula given by Eq. (20) for the values entering in the contact equations is given for the basic potentials of Eqs. (18), (19) on a cylindrical surface of the radius r . The components are determined by the first-order basic polynomial $\boldsymbol{f}^{(j)}$, which is related to the polynomials of the asymptotic behavior at infinity by the following linear equations with unknown coefficients:

$$\boldsymbol{f}^{(j)}(P) = A_j\ \boldsymbol{f}^{(H)}(P) + B_j\,\boldsymbol{r}\,\mathrm{div}\,\boldsymbol{f}^{(H)}. \tag{21}$$

The potentials $\boldsymbol{f}_1$, $\boldsymbol{f}_2$, $\boldsymbol{f}_3$, $\boldsymbol{f}_4$ generate the following expansions associated with Eq. (20):

$$\boldsymbol{U} = \frac{(1-2\nu)\,\boldsymbol{f}^{(j)}}{2\mu(1-\nu)}, \quad \frac{\partial \boldsymbol{U}}{\partial r} = \frac{\boldsymbol{U}}{r}, \quad \boldsymbol{p} = r^{-1}\frac{(1-2\nu)\,\boldsymbol{f}^{(j)} + \nu\,(\boldsymbol{r}\,\mathrm{div}\,\boldsymbol{f}^{(j)})}{1-\nu};$$

$$\boldsymbol{U} = \frac{r^{-2}}{2\mu(1-\nu)}\left((1-2\nu)\,\boldsymbol{f}^{(j)} + \frac{\boldsymbol{r}\,(\boldsymbol{r}\,\boldsymbol{f}^{(j)})}{r^2}\right), \quad \frac{\partial \boldsymbol{U}}{\partial r} = -\frac{\boldsymbol{U}}{r},$$

$$\boldsymbol{p} = \frac{r^{-3}}{1-\nu}\left(\boldsymbol{f}^{(j)} + \nu\,(\boldsymbol{r}\,\mathrm{div}\,\boldsymbol{f}^{(j)}) - \frac{3\boldsymbol{r}\,(\boldsymbol{r}\,\boldsymbol{f}^{(j)})}{r^2}\right);$$

$$\boldsymbol{U} = -\frac{r^{-4}(3-2\nu)}{\mu(1-\nu)}\left(2\,\boldsymbol{f}^{(j)} + \boldsymbol{r}\,\mathrm{div}\,\boldsymbol{f}^{(j)} - \frac{4\boldsymbol{r}\,(\boldsymbol{r}\,\boldsymbol{f}^{(j)})}{r^2}\right), \quad \frac{\partial \boldsymbol{U}}{\partial r} = -\frac{3\boldsymbol{U}}{r},$$

$$\boldsymbol{p} = \frac{r^{-5}6(3-2\nu)}{1-\nu}\left(2\,\boldsymbol{f}^{(j)} + \boldsymbol{r}\,\mathrm{div}\,\boldsymbol{f}^{(j)} - \frac{4\boldsymbol{r}\,(\boldsymbol{r}\,\boldsymbol{f}^{(j)})}{r^2}\right);$$

$$\boldsymbol{U} = -\frac{2r^2}{\mu(1-\nu)}\left((3-2\nu)\,\boldsymbol{f}^{(j)} - \nu\,(\boldsymbol{r}\,\mathrm{div}\,\boldsymbol{f}^{(j)}) - (3-4\nu)\frac{\boldsymbol{r}\,(\boldsymbol{r}\,\boldsymbol{f}^{(j)})}{r^2}\right),$$

$$\frac{\partial \boldsymbol{U}}{\partial r} = \frac{3\boldsymbol{U}}{r}, \quad \boldsymbol{p} = -\frac{12r}{1-\nu}\left(\boldsymbol{f}_n^{(j)} - \frac{\boldsymbol{r}\,(\boldsymbol{r}\,\boldsymbol{f}_n^{(j)})}{r^2}\right).$$

Analogous forms for the expansions associated with Eq. (20) for potentials given by Eq. (19) of Helmholtz type are obtained by using the following recurrence relations, valid for the radial multipliers $h_n(r)$ of arbitrary order:

$$r^2 h_{n+2} + 2(n+1)h_{n+1} - \kappa^2 h_n = 0,$$

where $h_{n+1}(r) = h_n'(r)/r$ and $\kappa^2 = C/\mu$. The same relations hold for $h_n^*(r)$ with replacing κ^2 by $\left(\kappa^*\right)^2 = C/k$, $k = 2\mu + \lambda$.

The potential $\boldsymbol{f}_5^*$ in Eq. (19) generates the following expansions of the form of Eq. (20):

$$\boldsymbol{u} = \frac{h_2^*}{C}\left(2\,\boldsymbol{f}^{(j)} + \boldsymbol{r}\,\mathrm{div}\,\boldsymbol{f}^{(j)}\right) + \frac{h_3^*}{C}\boldsymbol{r}\,(\boldsymbol{r}\,\boldsymbol{f}^{(j)}),$$

$$\frac{\partial \boldsymbol{u}}{\partial r} = r^{-1}\left[\left(\frac{h_1^*}{k} - \frac{3h_2^*}{C}\right)\left(2\boldsymbol{f}^{(j)} + \boldsymbol{r}\ \mathrm{div}\ \boldsymbol{f}^{(j)}\right) + \left(\frac{h_2^*}{k} - \frac{3h_3^*}{C}\right)\boldsymbol{r}\,(\boldsymbol{r}\boldsymbol{f}^{(j)})\right],$$

$$\hat{\boldsymbol{p}}(\boldsymbol{u}) = -r^{-1}\left[2\left(\frac{\lambda}{k}h_1^* + \frac{3\mu - 2\lambda}{C}h_2^*\right)\boldsymbol{f}^{(j)} + (6\mu + \lambda)\left(\frac{h_0^*}{k} - \frac{2h_1^*}{C}\right)\frac{\boldsymbol{r}\,\mathrm{div}\,\boldsymbol{f}^{(j)}}{r^2} + \right.$$
$$\left. + \left(\frac{4\mu - \lambda}{k}h_1^* - \frac{2(9\mu - \lambda)}{C}h_2^*\right)\frac{\boldsymbol{r}\,(\boldsymbol{r}\boldsymbol{f}^{(j)})}{r^2}\right],$$

whereas the potential $\boldsymbol{f}_6^*$ generates the same components by replacing h_n^* with $\hat{h}_n^*$. For the potential $\boldsymbol{f}_7$ we have:

$$\boldsymbol{u} = \left(\frac{h_1}{\mu} - \frac{2h_2}{C}\right)\boldsymbol{f}^{(j)} - \frac{h_2}{C}\boldsymbol{r}\ \mathrm{div}\ \boldsymbol{f}^{(j)} - \frac{h_3}{C}\boldsymbol{r}\,(\boldsymbol{r}\boldsymbol{f}^{(j)}),$$

$$\frac{\partial \boldsymbol{u}}{\partial r} = -\frac{r^{-1}}{\mu}\left[\left(h_1 - \left(r^2 + \frac{6\mu}{C}\right)h_2\right)\boldsymbol{f}^{(j)} + \left(h_1 - \frac{3\mu h_2}{C}\right)\boldsymbol{r}\ \mathrm{div}\ \boldsymbol{f}^{(j)} + \left(h_2 - \frac{3\mu h_3}{C}\right)\boldsymbol{r}\,(\boldsymbol{r}\boldsymbol{f}^{(j)})\right],$$

$$\hat{\boldsymbol{p}}(\boldsymbol{u}) = -r^{-1}\left[\left(3h_1 - \frac{2(3\mu - 2\lambda)}{C}h_2\right)\boldsymbol{f}^{(j)} - \left(5h_1 - \frac{2(9\mu - \lambda)}{C}h_2\right)\frac{\boldsymbol{r}\,(\boldsymbol{r}\boldsymbol{f}_n^{(j)})}{r^2} - \right.$$
$$\left. - \left(\frac{6\mu + \lambda}{\mu}h_0 - \left(r^2 + \frac{2(6\mu + \lambda))}{C}\right)h_1\right)\frac{\boldsymbol{r}\ \mathrm{div}\ \boldsymbol{f}^{(j)}}{r^2}\right],$$

whereas the potential $\boldsymbol{f}_8$ generates exactly the same components by replacing h_n with $\hat{h}_n$.

Thus, in each subdomain $G_j = \{r_j < r < r_{j+1}\}$, the solution is determined in the following form based on the basic potentials given by Eqs. (18), (19) and (21) with a sufficient number of degrees of freedom corresponding to the necessary number of vector contact conditions given by Eqs. (15), (16) in the form of Eq. (20):

$$\boldsymbol{f}_0(P) = A_j\,\boldsymbol{f}^{(H)} + B_j\,\boldsymbol{r}\,\mathrm{div}\,\boldsymbol{f}^{(H)} + C_j\,r^6\nabla\,\mathrm{div}\left(r^{-2}\boldsymbol{f}^{(H)}\right) + \\ + r^{-2}\left(\hat{A}_j\,\boldsymbol{f}^{(H)} + \hat{B}_j\,\boldsymbol{r}\,\mathrm{div}\,\boldsymbol{f}^{(H)}\right) + \hat{C}_j\,\nabla\,\mathrm{div}\left(r^{-2}\boldsymbol{f}^{(H)}\right), \tag{22}$$

$$\boldsymbol{f}^*(P) = h_1^*\left(A_j^*\,\boldsymbol{f}^{(H)} + B_j^*\,\boldsymbol{r}\,\mathrm{div}\,\boldsymbol{f}^{(H)}\right) + \hat{h}_1^*\left(\hat{A}_j^*\,\boldsymbol{f}^{(H)} + \hat{B}_j^*\,\boldsymbol{r}\,\mathrm{div}\,\boldsymbol{f}^{(H)}\right), \tag{23}$$

$$\boldsymbol{f}(P) = C_j^*\,h_1\,\boldsymbol{f}^{(H)} + \hat{C}_j^*\,\hat{h}_1\,\boldsymbol{f}^{(H)}. \tag{24}$$

This is the most general form of potentials for solving the generalized Eshelby problem in the multilayer cylinder with first order conditions at infinity. Here we assume that the potentials $\boldsymbol{f}_3$, $\boldsymbol{f}_4$ generate a zero deformation state for the planar expansion defined by the polynomials $\boldsymbol{r}\,\mathrm{div}\,\boldsymbol{f}^{(j)}$. The coefficients A_j, B_j, C_j, A_j^*, B_j^*, C_j^* are associated with the regular part of displacements increasing at infinity, and the coefficients $\hat{A}_j$, $\hat{B}_j$, $\hat{C}_j$, $\hat{A}_j^*$, $\hat{B}_j^*$, $\hat{C}_j^*$ are associated with the singular part of displacements decreasing at infinity. There are no singular potentials in

the domain G_I for a base inclusion. On the contrary, there are singular potentials only in the domain G_H corresponding to a material with equivalent characteristics.

For the four-cylinder model considered in this paper, the total number of unknown coefficients is 24: the regular coefficients A_j, B_j, C_j, $j=0,1,2$; the singular coefficients $\hat{A}_j$, $\hat{B}_j$, $\hat{C}_j$, $j=1,2,3$; and also the coefficients A_j^*, B_j^*, C_j^*, $\hat{A}_j^*$, $\hat{B}_j^*$, $\hat{C}_j^*$, $j=1$, corresponding to the cohesion field in the fuzzy layer. The indices $j=0,1,2,3$ are associated with the domains G_I, G_L, G_M and G_H, respectively. The total number of unknown coefficients coincides with the number of contact equations on the interface boundaries.

The method of constructing the solutions, which was realized in this section for linear displacement fields at infinity (the function $\boldsymbol{f}^{(H)}$ in Eqs. (22) – (24) is a linear harmonic polynomial), is a general method and remains valid for the case when the displacement field far from inclusions is determined by a Harmonic polynomial of arbitrary degree *n*. In this case, the appropriate solutions are also effective to approximate the deformations for a periodic cell with multilayered inclusions by using the method of asymptotic homogenization, when it is required to take into account the interaction of closely located spherical and cylindrical inclusions.

5. Determination of the effective moduli of the fuzzy fiber composite by the Eshelby-Christensen method

The determination of the effective characteristics of an inhomogeneous composite viewed as a multilayered four-cylinder body of Fig.1 is based on the analytical solution of generalized Eshelby-Christensen method. The criterion for deducing effective properties is the Eshelby energy principle [24, 25], which assumes a zero energy increment when a homogeneous body with effective characteristics is replaced by its inhomogeneous multilayered counterpart with a "fuzzy" whiskers layer introduced to improve adhesion. This, in turn, introduces an additional equation in the generalized Eshelby problem for the characteristics of the surrounding matrix which are considered as unknown variables. To determine different characteristics, different stress-strain states at infinity are assumed. Thus, in order to calculate the effective modulus $K_H=\left(C_{1111}+C_{2222}\right)/2$, where C_{ijkl} is the stiffness matrix, the body is stretched in the transverse direction with the displacements defined by the function $\boldsymbol{f}^{(H)}=\{x,y,0\}$. To compute the effective shear modulus $\mu_H^{(1)}=C_{1212}$ in the same direction, the body is subjected to a pure shear deformation with the displacements defined by the function $\boldsymbol{f}^{(H)}=\{x,-y,0\}$. And, in order to compute the longitudinal modulus in tension/compression $k_H=C_{3333}$ and, at the same time, the

transverse Lamé modulus $\lambda_H^{(2)} = C_{1133} = C_{2233}$, the body is subjected to a tensile deformation $\boldsymbol{f}^{(H)} = \{0, 0, z\}$ along this axis. Finally, to calculate the shear modulus $\mu_H^{(2)} = C_{1313} = C_{2323}$ in the longitudinal direction, the body is subjected to a simple shear deformation $\boldsymbol{f}^{(H)} = \{0, 0, x\}$ along the axis of the multilayer cylinder. This approach takes into account the anisotropy of material, as expressed through the different moduli for the various deformation processes.

Applying Eshelby's energy principle to all these cases, we obtain an additional equation $\hat{A}_3 = \hat{B}_3 = 0$ for the coefficients in the potentials given by Eqs. (22) – (24) for regions $G_0 = G_I$, $G_1 = G_L$, $G_2 = G_M$ and $G_3 = G_H$. This results to a system of linear algebraic equations with respect to the coefficients entering in the representations given by Eqs. (22) – (24) and the moduli K_H, $\mu_H^{(1)}$, $\lambda_H^{(2)}$, $\mu_H^{(2)}$. The effective modulus k_H is determined by the mixture rule.

Let us now consider the problem of determining the effective modulus $K_H = \left(C_{1111} + C_{2222}\right)/2$. After normalizing and transforming the general system of equations for the basic function $\boldsymbol{f}^{(H)} = \{x, y, 0\}$ and taking into account the condition $\hat{A}_3 = 0$, we obtain a system of 8×8 linear equations for determining the normalized coefficients and K_H:

$$A_j^н = A_j \frac{k_H}{k_j}, \quad \hat{A}_j^н = \hat{A}_j r_{j-1}^{-2} \frac{k_H}{\mu_j}, \quad j = 0,1,2, \quad A_1^{*н} = A_1^* \frac{k_H}{k_L}, \quad \hat{A}_1^{*н} = \hat{A}_1^* \frac{k_H}{k_L};$$

$$A_0^н = A_1^н + \hat{A}_1^н - (A_1^{*н} h_{1,L}^* + \hat{A}_1^{*н} \hat{h}_{1,L}^*), \qquad A_0^н = 2\hat{A}_1^н + r_0^2 (A_1^{*н} h_{2,L}^* + \hat{A}_1^{*н} \hat{h}_{2,L}^*),$$

$$(K_I + \mu_L) A_0^н = k_L A_1^н + \frac{k_L}{2} (A_1^{*н} h_{1,L}^* + \hat{A}_1^{*н} \hat{h}_{1,L}^*);$$

$$A_1^н + (r_0/r_1)^2 \hat{A}_1^н - (A_1^{*н} \%{h}_{1,L} + \hat{A}_1^{*н} \hat{\%}{h}_{1,L}) = A_2^н + \hat{A}_2^н, \qquad (r_0/r_1)^2 2\hat{A}_1^н + r_1^2 (A_1^{*н} \%{h}_{2,L} + \hat{A}_1^{*н} \hat{\%}{h}_{2,L}) = A_2^н + \hat{A}_2^н,$$

$$k_L A_1^н + \frac{k_L}{2} (A_1^{*н} \%{h}_{1,L} + \hat{A}_1^{*н} \hat{\%}{h}_{1,L}) = (K_M + \mu_L) A_2^н + (\mu_L - \mu_M) \hat{A}_2^н;$$

$$A_2^н + (r_1/r_2)^2 \hat{A}_2^н = 1, \qquad k_M A_2^н = K_H - \mu_M.$$

Here $h_{1,L}^*$, $\hat{h}_{1,L}^*$, $h_{2,L}^*$, $\hat{h}_{2,L}^*$ are the values of radial functions for $r = r_0$ and $\kappa^* = \sqrt{C_L/(2\mu_L + \lambda_L)}$, and $\%{h}_{1,L}$, $\%{h}_{2,L}$, $\hat{\%}{h}_{1,L}$, $\hat{\%}{h}_{2,L}$ are the values of radial functions for $r = r_1$ and the same κ^*. The effective modulus K_H is obtained directly from an 8×8 system of linear algebraic equations. For the limiting case $C_L \to \infty$, corresponding to a zero cohesion field in the fuzzy layer, the system of equations is simplified, and the coefficients A_1^* and $\hat{A}_1^*$ are assumed to be zero. The resulting system is solved in an explicit form:

$$K_H = K_M + \frac{c_0 D_H}{1+(1-c_0)\,D_H/k_M}, \tag{25}$$

$$D_H = \frac{K_I - K_M - (1-c_1)(K_I - K_L)(1+(K_M - K_L)/k_L)}{1+(1-c_1)(K_I - K_L)/k_L}, \tag{26}$$

where $c_0 = (r_1/r_2)^2$, $c_1 = (r_0/r_1)^2$.

Further reduction of the system of equations to a 4×4 for a three-cylinder body allows to determine the effective modulus K_H, which corresponds to the case $c_1 = 1$ in Eqs. (25) and (26):

$$K_H = K_M + \frac{c_0 (K_I - K_M)}{1+(1-c_0)(K_I - K_M)/k_M}, \tag{27}$$

where $c_0 = (r_1/r_2)^2$ is the volume fraction, and $k_M = K_M + \mu_M$.

Next, let us consider the problem of determining the effective modulus $k_H = C_{3333}$ and $\lambda_H^{(2)} = C_{1133} = C_{2233}$ by focusing on a uniaxial deformation $\boldsymbol{f}^{(H)} = \{0, 0, z\}$. In the direction of the axis z the cohesive field does not operate, and we assume that the effective modulus k_H is determined by the rule of the mixtures. However, in the transverse direction it acts through a stress field $\{\sigma_{11}, \sigma_{22}\}$, which determines the transverse modulus $\lambda_H^{(2)}$. Transforming the general system of equations that solves the generalized Eshelby problem for $\boldsymbol{f}^{(H)} = \{0, 0, z\}$ and assuming homogeneity of the deformation for the entire effective matrix, we obtain a system of 8×8 equations for determining $\lambda_H^{(2)}$:

$$A_j^{\prime\prime} = \frac{2A_j}{k_j}, \quad \hat{A}_j^{\prime\prime} = \frac{2\hat{A}_j r_{j-1}^{-2}}{\mu_j}, \quad j = 0,1,2, \quad A_1^{*\prime\prime} = \frac{2A_1^*}{k_L}, \quad \hat{A}_1^{*\prime\prime} = \frac{2\hat{A}_1^*}{k_L};$$

$$A_0^{\prime\prime} = A_1^{\prime\prime} + \hat{A}_1^{\prime\prime} - (A_1^{*\prime\prime} h_{1,L}^* + \hat{A}_1^{*\prime\prime} \hat{h}_{1,L}^*), \qquad A_0^{\prime\prime} = 2\hat{A}_1^{\prime\prime} + r_0^2 (A_1^{*\prime\prime} h_{2,L}^* + \hat{A}_1^{*\prime\prime} \hat{h}_{2,L}^*),$$

$$(K_I + \mu_L) A_0^{\prime\prime} + \lambda_I = k_L A_1^{\prime\prime} + \frac{k_L}{2}(A_1^{*\prime\prime} h_{1,L}^* + \hat{A}_1^{*\prime\prime} \hat{h}_{1,L}^*) + \lambda_L;$$

$$A_1^{\prime\prime} + (r_0/r_1)^2 \hat{A}_1^{\prime\prime} - (A_1^{*\prime\prime} h_{1,L}^{\%} + \hat{A}_1^{*\prime\prime} \hat{h}_{1,L}^{\%}) = A_2^{\prime\prime} + \hat{A}_2^{\prime\prime}, \qquad (r_0/r_1)^2 2\hat{A}_1^{\prime\prime} + r_1^2 (A_1^{*\prime\prime} h_{2,L}^{\%} + \hat{A}_1^{*\prime\prime} \hat{h}_{2,L}^{\%}) = A_2^{\prime\prime} + \hat{A}_2^{\prime\prime},$$

$$k_L A_1^{\prime\prime} + \frac{k_L}{2}(A_1^{*\prime\prime} h_{1,L}^{\%} + \hat{A}_1^{*\prime\prime} \hat{h}_{1,L}^{\%}) + \lambda_L = (K_M + \mu_L) A_2^{\prime\prime} + (\mu_L - \mu_M) \hat{A}_2^{\prime\prime} + \lambda_M;$$

$$A_2^{\prime\prime} + (r_1/r_2)^2 \hat{A}_2^{\prime\prime} = 0, \qquad k_M A_2^{\prime\prime} + \lambda_M = \lambda_H^{(2)}.$$

For the limiting case $C_L \to \infty$, corresponding to a “classical” interface layer, the coefficients A_1^* and $\hat{A}_1^*$ are assumed to be equal to zero, and the system of relevant equations reduces to 6×6 which is solved in an explicit form:

$$\lambda_H^{(2)} = \lambda_M + c_0 \frac{1+(1-c_1)(K_I-K_L)/k_L}{1+(1-c_0)(K_L-K_M)/k_M}\left(\lambda_L-\lambda_M+\frac{c_1(\lambda_I-\lambda_L)}{1+(1-c_1)(K_I-K_L)/k_L}\right)\times$$
$$\times\left[1+(K_I-K_L)/k_L\left(1-c_1\frac{c_0+(1-c_0)(\mu_M-\mu_L)/k_M}{1+(1-c_0)(K_L-K_M)/k_M}\right)\right]^{-1}, \tag{28}$$

where $c_0=(r_1/r_2)^2$, $c_1=(r_0/r_1)^2$. The "classical" three-cylinder model corresponds to the case $c_1=1$ in Eq (28):

$$\lambda_H^{(2)} = \lambda_M + \frac{c_0(\lambda_I-\lambda_M)}{1+(1-c_0)(K_I-K_M)/k_M}. \tag{29}$$

The problem of determining the effective modulus $\mu_H^{(2)}=C_{1313}=C_{2323}$ in the direction along the axis of the cylinder is determined on the basis of a simple shear deformation in the longitudinal direction $\boldsymbol{f}_0^{(H)}=\{0,0,x\}$. The system of equations corresponding to this case is as follows:

$$A_j^{\prime\prime}=A_j\frac{\mu_H}{\mu_j},\quad \hat{A}_j^{\prime\prime}=\hat{A}_j r_{j-1}^{-2}\frac{\mu_H}{\mu_j},\quad j=0,1,2,\quad C_1^{*\prime\prime}=C_1^*\frac{\mu_H}{\mu_L},\quad \hat{C}_1^{*\prime\prime}=\hat{C}_1^*\frac{\mu_H}{\mu_L};$$

$$A_0^{\prime\prime}=A_1^{\prime\prime}+\hat{A}_1^{\prime\prime}-(C_1^{*\prime\prime}h_{1,L}+\hat{C}_1^{*\prime\prime}\hat{h}_{1,L}),\qquad A_0^{\prime\prime}=2\hat{A}_1^{\prime\prime}+r_0^2(C_1^{*\prime\prime}h_{2,L}+\hat{C}_1^{*\prime\prime}\hat{h}_{2,L}),$$

$$\mu_I A_0^{\prime\prime}=\mu_L(A_1^{\prime\prime}-\hat{A}_1^{\prime\prime});$$

$$A_1^{\prime\prime}+(r_0/r_1)^2\hat{A}_1^{\prime\prime}-(C_1^{*\prime\prime}h_{1,L}^{\%}+\hat{C}_1^{*\prime\prime}\hat{h}_{1,L}^{\%})=A_2^{\prime\prime}+\hat{A}_2^{\prime\prime},\qquad (r_0/r_1)^2 2\hat{A}_1^{\prime\prime}+r_1^2(C_1^{*\prime\prime}h_{2,L}^{\%}+\hat{C}_1^{*\prime\prime}\hat{h}_{2,L}^{\%})=A_2^{\prime\prime}+\hat{A}_2^{\prime\prime},$$

$$\mu_L\left(A_1^{\prime\prime}-(r_0/r_1)^2\hat{A}_1^{\prime\prime}\right)=\mu_M(A_2^{\prime\prime}-\hat{A}_2^{\prime\prime});$$

$$A_2^{\prime\prime}+(r_1/r_2)^2\hat{A}_2^{\prime\prime}=1,\qquad \mu_M\left(A_2^{\prime\prime}-(r_1/r_2)^2\hat{A}_2^{\prime\prime}\right)=\mu_H^{(2)}.$$

Thus, in order to determine $\mu_H^{(2)}$, we solve a system of 8×8 equations similar to previous cases. For the limiting case $C_L\to\infty$ corresponding to a "classical" interface layer, the effective modulus $\mu_H^{(2)}$ is determined by the following formulas:

$$\mu_H^{(2)} = \mu_M + \frac{c_0 D_H}{1+(1-c_0)\,D_H/(2\mu_M)}, \tag{30}$$

$$D_H = \frac{\mu_I-\mu_M-(1-c_1)(\mu_I-\mu_L)(1+(\mu_M-\mu_L)/(2\mu_L))}{1+(1-c_1)(\mu_I-\mu_L)/(2\mu_L)}, \tag{31}$$

where $c_0=(r_1/r_2)^2$, $c_1=(r_0/r_1)^2$. The three-cylinder "classical" model corresponds to the case $c_1=1$ in Eqs. (30) and (31):

$$\mu_H^{(2)} = \mu_M + \frac{c_0(\mu_I-\mu_M)}{1+(1-c_0)(\mu_I-\mu_M)/(2\mu_M)}. \tag{32}$$

The problem of determining the effective modulus $\mu_H^{(1)} = C_{1212}$ in the transverse direction is based on considering a state of pure shear deformation $\boldsymbol{f}^{(H)} = \{x, -y, 0\}$. This reduces to the determination of all coefficients in Eqs. (22) – (24) (except B_j and $\hat{B}_j$, since div $\boldsymbol{f}^{(H)} = 0$). Transforming the general system of equations of the generalized Eshelby problem in order to display the shear modulus in the transverse direction, we obtain a system of 16×16 linear algebraic equations containing the unknown coefficient $\hat{A}_3$ and the unknown modulus $\mu_H^{(1)} = C_{1212}$. According to the self-consistency condition, the coefficient $\hat{A}_3$ must be zero. To fulfill this condition, we use an iterative process in which we change the modulus $\mu_H^{(1)}$ until the condition $\hat{A}_3 = 0$ is satisfied. This gives the effective value of the shear modulus $\mu_H^{(1)}$. The dependence of the coefficient $\hat{A}_3$ on $\mu_H^{(1)}$ is nonlinear. Therefore, we obtain a transcendental equation for $\mu_H^{(1)}$, which is solved by an iterative method, unlike the previous cases, in which the effective moduli K_H, k_H, $\mu_H^{(2)}$ and $\lambda_H^{(2)}$ were found from the solution of a system of linear algebraic equations.

As a result, we obtain all necessary characteristics K_H, $\mu_H^{(1)}$, k_H, $\lambda_H^{(2)}$ and $\mu_H^{(2)}$ for the unidirectional fiber composites with “fuzzy” layers by solving linear systems of equations of dimensions 8×8 and 16×16. In particular, for the “classical” three-cylinder model, Eqs. (27), (29) and (32), allow to estimate the characteristics of the fuzzy layer itself, which is considered in this case as a set of elementary fibers grown on the base fiber.

6. Numerical results

We consider a composite reinforced with carbon fibers T650 of diameter $D = 5\,\mu\text{m}$ with a layer of whiskers of width $l_0 = 2\,\mu\text{m}$. The values of the carbon fiber parameters are assumed as follows: longitudinal Young's modulus $E_1 = 241\,\text{GPa}$, Young's transverse modulus $E_2 = 14.5\,\text{GPa}$, shear modulus along the fiber axis $G_{13} = 22.8\,\text{GPa}$, shear modulus in the transverse direction $G_{12} = 4.8\,\text{GPa}$, Poisson's ratio $\nu_{12} = 0.27$. The “whisker” layer consists of carbon nanotubes (CNT) of diameter $d = 0.85\,\text{nm}$ and length $L = 2000\,\text{nm}$, uniformly covering the surface of the base fiber. The average volume concentration of CNTs in the entire layer of whiskers (which determines the distance between nanotubes on the surface of the base fiber) is equal to $c_0 = 42.17\,\%$. The following CNT parameters are assumed for the calculations: $E = 1100\,\text{GPa}$, $\nu = 0.14$. The matrix is assumed to be an epoxy resin with parameters $E_M = 3\,\text{GPa}$, $\nu_M = 0.3$.

The average density c_0 of CNT in the "whisker" layer and the total number N in each section are assumed to be equal:

$$c_0 = \frac{\pi D}{4(D+L)}\left(\frac{d}{h}\right)^2 100\%, \qquad N = \frac{\pi D}{h},$$

where h is the distance between CNT tubes on the surface of base fiber.

The assumed geometry of the whisker package, based on the average density $c_0 = 42.17\%$, leads to the conclusion that the distance between the CNT tubes on the base surface is equal to $h = 0.98$ nm and the total number of tubes in each section is $N = 16022$. As a result, for the density of CNT packing on a parallel surface, located at the distance x from the base surface, we obtain the formula:

$$c(x) = \frac{Nd^2}{4h(D+2x)}100\%. \tag{33}$$

To assess the effective characteristics $\left(K_L,\ \lambda_L^{(2)},\ \mu_L^{(2)}\right)$ of the whisker layer, we use the formulas of the self-consistent Eshelby-Christensen model for a three-cylinder body given by Eqs. (27), (29) and (32) with parameters corresponding to the chosen direction, along with the rule of mixtures formula for the k_L and the iterative algorithm for $\mu_L^{(1)}$. As a result, the longitudinal Young's modulus of the whisker layer E_{1L} and the longitudinal shear modulus G_{13L} are determined by the formulas:

$$E_{1L} = \frac{k_L(1+\nu_L)(1-2\nu_L)}{1-\nu_L}, \qquad G_{13L} = \mu_L^{(2)}, \tag{34}$$

where $\nu_L = \lambda_L^{(2)}/(2K_L)$ is the effective Poisson's ratio of the whisker layer. Similarly, the transverse Young's modulus of the whisker layer E_{2L} and the transverse shear modulus G_{12L} are determined by the formulas:

$$E_{2L} = \frac{\mu_L^{(1)}(3K_L - \mu_L^{(1)})}{K_L}, \qquad G_{12L} = \mu_L^{(1)}. \tag{35}$$

This corresponds to a recalculation of the Young's modulus through the comprehensive planar expansion modulus based on the hypothesis of an orthotropic effective layer.

However, for a more accurate evaluation of the effective characteristics of the whisker layer – which takes into account the variability of its characteristics with the distance from the base fiber – a calculation with a variable value of the volume concentration was carried out, taking into account the estimate given by Eq. (33), depending on the distance χ from the surface of the base fiber. A similar calculation was made in [29] by the method of asymptotic

homogenization, and Fig.2 presents a comparison of these results. Note that the work of [29] is perhaps the only fundamental work known to the authors, which provides an accurate study of the effect of CNTs nanostructures density near the fiber surface on the effective interfacial layer properties for “fuzzy” composite systems. The curves shown in Fig.2 represent a satisfactory agreement between the results of analytical modeling and the results obtained by the method of asymptotic homogenization. Analytical solutions give a somewhat better understating of the effective characteristics because they take into account the effects of anisotropy, related to the change in the density of the nanostructure on the distance x from the base surface of the fiber.

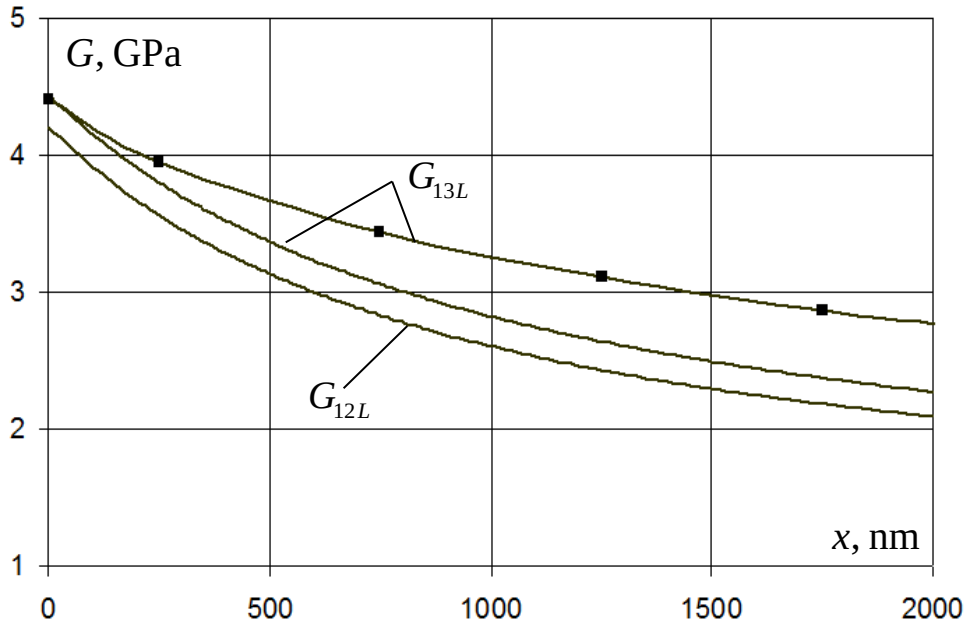

Fig.2. Variable effective characteristics of the shear of interphase layer, depending on the distance from the base fiber: G_{13L} is the longitudinal shear modulus, G_{12L} is the transverse shear modulus; -■- are results of [29].

Next, the effective properties of the fiber composite as a whole are studied. For this case, consideration of the effective characteristics of the whisker layer, was carried out for the average value of the volume concentration $c_0 = 42.17\%$. As a result, the following values were obtained: $E_{1L} = 6.64$ GPa, $G_{13L} = 2.6$ GPa, $E_{2L} = 428.2$ GPa, $G_{13L} = 2.82$ GPa, $\nu_L = 0.219$. These were used to calculate the effective characteristics of the composite material using the gradient Eshelby-Christensen model. In reality, the interface layer has variable characteristics in the direction of the radial coordinate, i.e. it is a functionally-graded material. In order to consider such a “graded” nature, we take into account the correspondence between the solutions of non-local theories of elasticity and the solutions of classical elasticity for materials with functionally-graded properties [23, 24]. We use, for this purpose, a gradient model for the interphase layer,

and determine the effective properties of a fiber composite, by employing the generalized self-consistent method of Eshelby [25, 26].

Figs. 3-6 show the results of the calculation for the effective characteristics of a unidirectional composite material with fuzzy or whiskered fibers depending on the volume concentration of the base fibers c_0. The limiting concentration at which the layers touch is calculated by the formula $c = \pi/4\left(1+2l_0/D\right)^{-2}$ and is equal to the value $c = 0.25$. The scale parameter C was chosen in the calculations in such a way that it gives the value $\kappa^* = \sqrt{C/k_L} = 2.5$, i.e. $C = 6.25k_L$. This corresponds to effective parameters (with a cohesive field), vanishing approximately in the middle of the whisker layer. In the figures, this dependence is shown by a thick line. The calculation of the effective characteristics by the "classical" model corresponds to the limiting value of the parameter $C \to \infty$. In the figures this dependence is shown by a thin line, and the calculation for the intermediate value $C = 25k_L$ is also shown in the figures by a thin line.

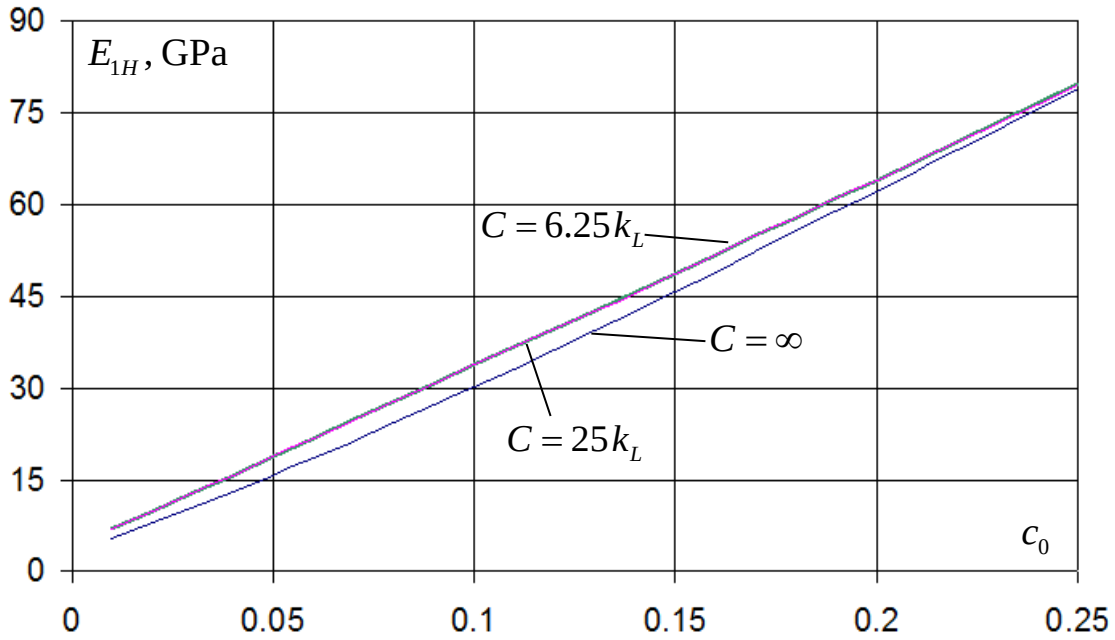

Fig. 3. Effective Young's modulus E_{1H} in the longitudinal direction.

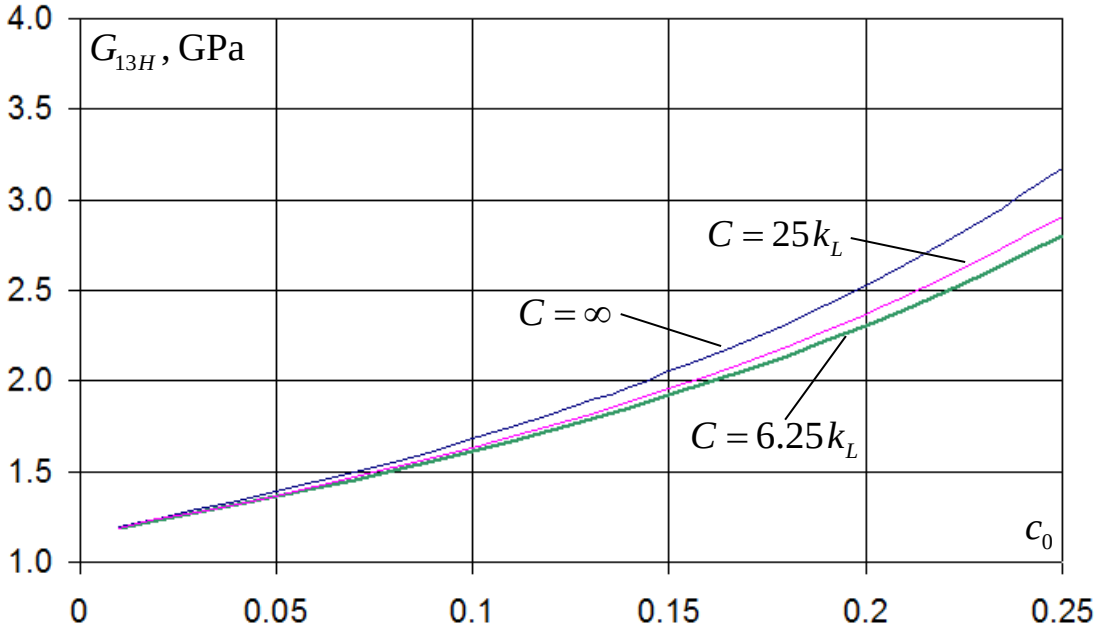

Fig. 4. Effective shear modulus G_{13H} in the longitudinal direction.

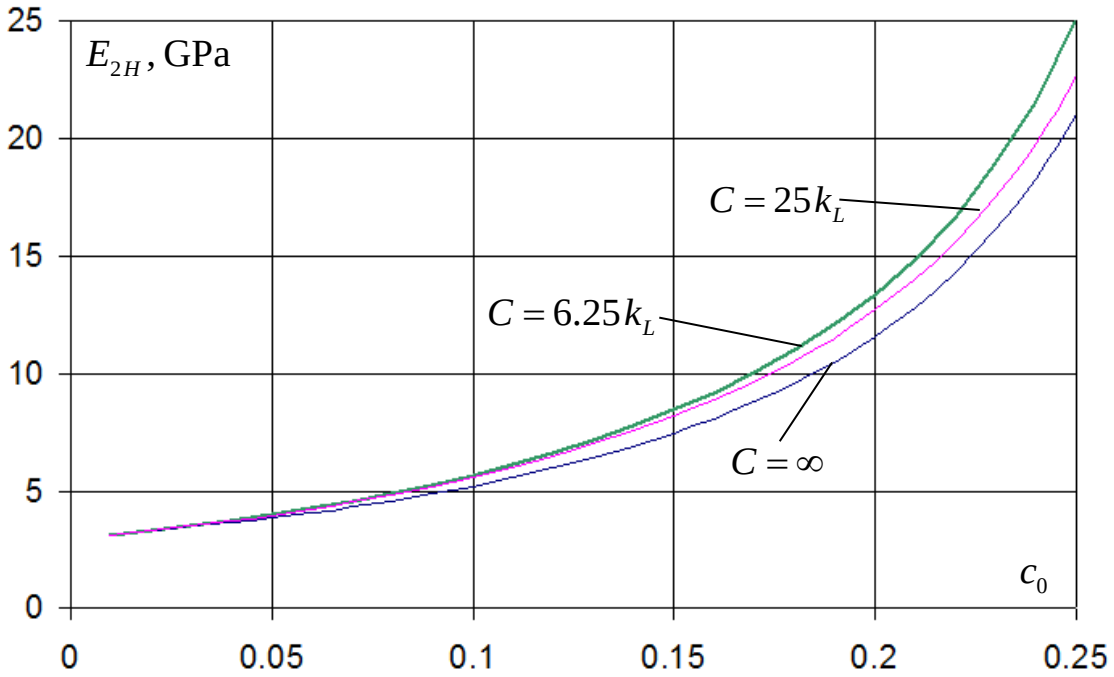

Fig. 5. Effective Young's modulus E_{2H} in the transverse direction.

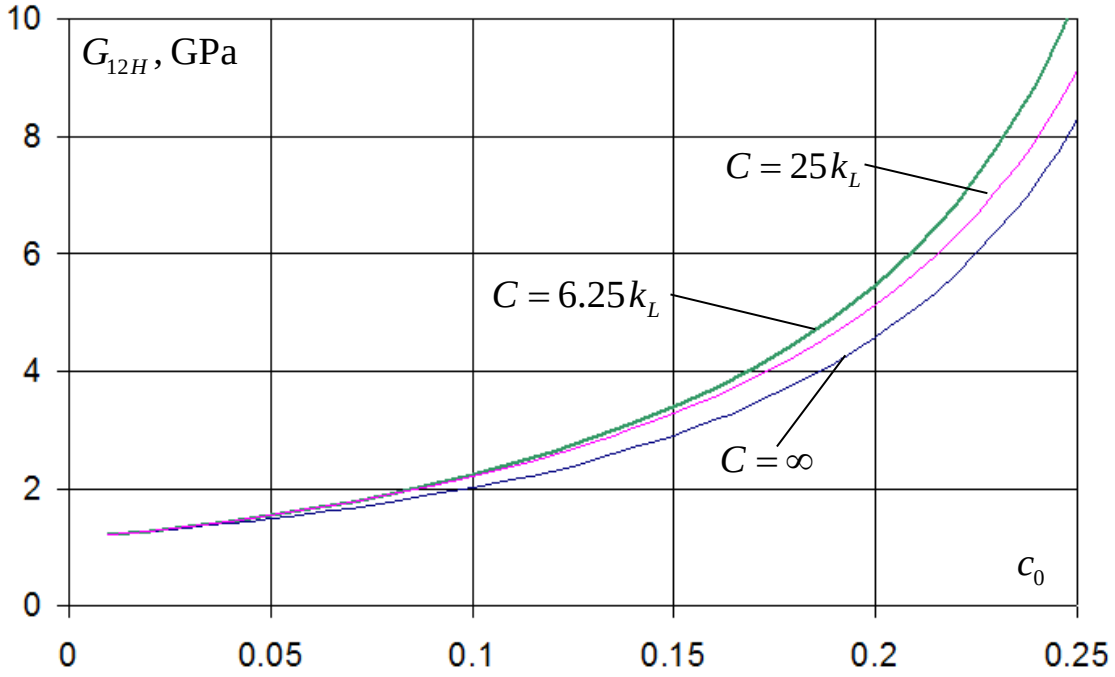

Fig. 6. Effective shear modulus G_{12H} in the transverse direction.

To validate the proposed analytical method based on the GradEla model utilizing the concept of a CNT whisker layer, reference is made to previous results on analytical and numerical modeling of "fuzzy" composites. In estimating the properties of the bristled interphase layer, three different procedures were adopted by the authors of [29]: the asymptotic homogenization self-consistent approach, the Mori–Tanaka scheme and the Eshelby self-consistent method [30]. Their results revealed that the transverse and shear properties of a fuzzy fiber composite are strongly influenced by the presence of CNTs, while the effect on the axial Young's modulus is marginal. These results were verified by comparison with numerical calculations based on the asymptotic expansion homogenization method [29]. It was shown that the numerical results of both [30] and [29] are in very good agreement with one another. In the present work the effect of length and volume fraction of CNTs on the effective characteristics of the whisker layer (see Fig.2) was also examined, establishing an agreement between our analytical results and the results obtained by the numerical method of asymptotic homogenization. This comparison also confirms that both of the aforementioned parameters significantly affect the overall properties of fuzzy fiber composites.

As far as comparisons with findings from experimental tests for fuzzy composites with CNT layers grown on the surface of the carbon fibers, reference is made to the work of [31]. Carbon fibers IM7 have the following mechanical characteristics [19]: $D = 5.2\,\mu\text{m}$, $E_1 = 256.76\,\text{GPa}$, $E_2 = 25.51\,\text{GPa}$, $G_{13} = 22.06\,\text{GPa}$, $G_{12} = 9.25\,\text{GPa}$, $\nu_{12} = 0.379$. The experimental data of [31] can be used to test the validity of the analytical approach proposed in

this paper for determining the effective moduli of a “fuzzy” composite based on the GradEla model. More specifically, as stated in [31], multilayer carbon nanotubes with diameter $d = 30$ nm , length $L = 100$ nm , and an average volume concentration $c_0 = 2\%$ were grown on the surface of the base fiber. With a volume fraction of the base fibers of 41%, the value $E_{2H} = 10.02$ GPa was obtained for the transverse effective modulus of the composite in the plane perpendicular to the base fibers. We established that for this case, the relative fraction of the viscous layer $L/D = 0.077$ is too small to have a significant effect on the value of the Young's transverse modulus calculated from the standard scheme which is equal to 6.34 GPa . This is well below the experimental value.

We, thus, suggest that the presence of CNTs has a modifying effect on the matrix itself, and in the above scheme, the matrix must be modeled by using the GradEla model employed in the present approach. This is consistent with the numerical approach used for the evaluation of the effective moduli in [31], where the effective characteristics of the viscous layer were extended to the entire matrix. Accordingly, as a result, we found that the value of the transverse modulus of the fiber composite $E_{2H} = 10.09$ GPa is reached when the scale parameter is equal to $C = 0.3k_M$ or $\kappa^* = \sqrt{C/k_M} = 0.5477$. This means that the modifying effect of the interphase layer due to CNTs extends over a distance approximately equal $0.9D = D/(2\kappa^*)$, where D is the diameter of base fiber. Thus, we showed that the method proposed in the present work gives physically consistent results and allows to describe adequately the experimentally obtained reinforcement effect for fuzzy composites.

7. Conclusions

The paper employed a generalized self-consistent Eshelby method that allows to obtain analytical estimates for the effective mechanical characteristics of fiber multilayered “fuzzy” composites. The fiber layers are assumed to be isotropic obeying classical elasticity, or described in the framework of gradient theories of elasticity. The proposed variant of the Eshelby method allows to obtain analytical estimates for the effective properties of composite structures for any homogeneous state at infinity. It also allows to take into account the variability of the density of carbon nanotubes (introduced on the surface of the carbon base fibers) with the radial coordinate in the vicinity of the fiber surface. It is shown that our analytical results are in agreement with numerical results obtained by the method of asymptotic homogenization. The evaluation of the effective properties of a fiber “fuzzy” composite is achieved by accounting for the variability of

the properties of the functional-graded interphase layer by using a nonlocal interphase layer model.

Acknowledgements

The authors are appreciative to Prof. Dr. A.N. Guz for discussions and insights on this topic. This work was carried out with support from MegaGrant Project No. 14.Z50.31.0039 to Togliatti State University.

REFERENCES

1. Lin Y, Ehlert GJ, Sodano HA. Increase interface strength in carbon fiber composites through a ZnO nanowire interphase. Advant Funct Mater 2009;19(16):2654-60.
2. Kim JK, Mai YW. Engineered interfaces in fiber reinforced composites. Elsevier Science Ltd 1998.
3. Guz IA, Rodger AA, Guz AN, Rushchitsky JJ. Predicting the properties of micro and nanocomposites: from the microwhiskers to the bristled nanocentipedes. Philos Trans R Soc A 2008;366:1827-33.
4. Gibson RF. A review of recent research on mechanics of multifunctional composite materials and structures. Compos Struct 2010;92:2793-810.
5. Kim H. Enhanced crack detection sensitivity of carbon fiber composites by carbon nanotubes directly grown on carbon fibers. Compos Part B 2014;60:284-91.
6. Talò M, Krause B, Pionteck J, Lanzara G, Lacarbonara W. An updated micromechanical model based on morphological characterization of carbon nanotube nanocomposites. Compos Part B 2017;115:70-78.
7. Boroujeni AY, Tehrani M, Nelson AJ, Al-Haik M. Hybrid carbon nanotube-carbon fiber composites with improved in-plane mechanical properties. Compos Part B 2014;66:475-83.
8. Kundawal SI, Ray MC. Effect of carbon nanotube waviness on the effective thermoelastic properties of a novel continuous fuzzy fiber reinforced composite. Compos Part B 2014;57:199-209.
9. Dai G, Mishnaevsky L. Carbone nanotube reinforced hybrid composites: Computational modelling of environmental fatigue and their usability for wind blades. Compos Part B 2015;78:349-60.
10. Gonzalez-Chi PI, Rodríguez-Uicab O, Martin-Barrera C, Uribe-Calderon J, Canche-Escamilla G, Yazdani-Pedram M, May-Pat A, Avilés F. Influence of aramid fiber treatment and carbon nanotubes on the interfacial strength of polypropylene hierarchical composites. Compos Part B 2017;122:16-22.

11. Skandani AA, Al-Haik M. Viscoplastic characterization and modeling of hybrid carbon fiber/carbon nanotubes reinforced composites. Compos Part B 2016;99:63-74.
12. Chatzigeorgiou G, Siedel GD, Lagoudas D. Effective mechanical properties of ‘‘fuzzy fiber’’ composites. Compos Part B 2012;43:2577-93.
13. Falzon BG, Hawkins SC, Huynh CP, Radjef R., Brown C. An investigation of mode I and mode II fracture toughness enhancement using aligned carbon nanotubes forests at the crack interface. Compos Struct 2013;106:65-73.
14. Mishnaevsky L. Nanostructured interfaces for enhancing mechanical properties of composites: Review of computational micromechanical studies. Compos Part B 2015;68:75-84.
15. Agnihotri P, Basu S, Kar KK. Effect of carbon nanotube length and density on the properties of carbon nanotubes coated carbon fiber/polyester composites. Carbon 2011;49:3098-106.
16. Steiner SA., Li R, Wardle BL. Circumventing the mechanochemical origins of strength loss in the synthesis of hierarchical carbon fibers. ACS Appl Mater Interfaces 2013;5(11):4892-903.
17. Guz IA, Rushchitsky JJ, Guz AN. Mechanical models for nanomaterials. Handbook of nanophysics – principles and methods, vol. 24. CRC 2011; 1-12.
18. Guz IA, Rushchitsky JJ, Guz AN. Effect of a special reinforcement on the elastic properties of micro- and nanocomposites with polymer matrix. Aeronautical J 2013;117(1196):1019-36.
19. Lurie SA, Minhat M. Application of generalized self-consistent method to predict effective elastic properties of bristled fiber composites. Compos Part B 2014;61:154-60.
20. Kundawal SI, Ray MC. Micromechanical analysis of fuzzy fiber reinforced composites. Int J Mech Mater Des 2011;7:149-66.
21. Lurie SA, Volkov-Bogorodskii DB, Leontiev A, Aifantis EC. Eshelby’s inclusion problem in the gradient theory of elasticity: Applications to composite materials. Int J Eng Sci 2011;49:1517-25.
22. Aifantis EC. Internal length gradient (ILG) mechanics across scales and disciplines. Adv Appl Mech 2016; 1-110
23. Lomakin EV, Lurie SA, Belov PA, Rabinskii LM. Modeling of the localy-functional properties of the material damaged by fields of defects. DAN RAS 2017;472(3):282-85.
24. Lurie SA, Volkov-Bogorodskii DB, Tuchkova NP. Exact solution of Eshelby-Christensen problem in gradient elasticity for composites with spherical inclusions. Acta Mech 2016;227:127-38.
25. Volkov-Bogorodskii DB, Lurie SA. Eshelby solution in gradient theory of elasticity for multilayered spherical inclusions. Mech of Solids 2016;2:32-50.

26. Gusev AA, Lurie SA. Symmetry conditions in strain gradient elasticity. Math Mech Solids 2015;1-9, doi: 10.1177/1081286515606960.
27. Aifantis KE, Willis JR. The role of interfaces in enhancing the yield strength of composites and polycrystals. J Mech Phys Solids 2005;53:1047-70.
28. Mindlin RD, Eshel NN. On first strain-gradient theories in linear elasticity. Int J Solids Struct 1968;4:109-24.
29. Chatzigeorgiou G, Efendiev Y, Lagoudas DC. Homogenization of aligned fuzzy fiber composites. Int J Solids Struct 2011;48(19):2668-80.
30. Seidel GD, Lagoudas DC. Micromechanical analysis of the effective elastic properties of carbon nanotube reinforced composites. Mech Mater 2006;38:884–907.
31. Kulkarni M, Carnahan D, Kulkarni K, Qian D, Abot JL. Elastic response of a carbon nanotube fiber reinforced polymeric composite: A numerical and experimental study. Compos Part B 2010;41:414-21.

Appendix 1. The general solution of the generalized Eshelby problem

A general system of the linear algebraic equations for the determination of the coefficients given by Eqs. (22) – (24) for the potentials of the solution in each subdomain G_I, G_L, G_M and G_H in the self-consistent model of four cylindrical bodies, is obtained by equating the radial multipliers in Eqs. (20), (21) for the contact conditions on the interface boundaries.

Separating in the contact conditions of Eqs. (20), (21) a normal component $\boldsymbol{r}(\boldsymbol{r}\,\boldsymbol{f}^{(H)})$ in a polynomial $\boldsymbol{f}^{(H)}$ (which determines the asymptotic behavior at infinity), the in-plane expansion component $\boldsymbol{r}\,\mathrm{div}\,\boldsymbol{f}^{(H)}$ and the tangential component $\boldsymbol{f}^{(H)}-\boldsymbol{r}(\boldsymbol{r}\,\boldsymbol{f}^{(H)})$, we obtain exactly three algebraic equations for each vector contact equation, by equating the radial multipliers in the specific form of Eq. (20) for the basic potentials given by Eqs. (18), (19), and dividing into groups of three algebraic equations, corresponding to the relevant contact conditions.

From the equality of displacements at the inclusion boundary $r=r_0$, the following equations can be derived:

$$A_0\frac{1-2\nu_I}{2\mu_I(1-\nu_I)}-C_0r_0^2\frac{4\nu_I}{\mu_I(1-\nu_I)}=A_1\frac{1-2\nu_L}{2\mu_L(1-\nu_L)}-C_1r_0^2\frac{4\nu_L}{\mu_L(1-\nu_L)}+\frac{\hat{A}_1r_0^{-2}}{\mu_L}+$$
$$+\hat{C}_1r_0^{-4}\frac{2(3-2\nu_L)}{\mu_L(1-\nu_L)}-A_1^*\left(\frac{h_{1,L}^*}{k_L}-\frac{2h_{2,L}^*}{C_L}\right)-C_1^*\frac{2h_{2,L}}{C_L}-\hat{A}_1^*\left(\frac{\hat{h}_{1,L}^*}{k_L}-\frac{2\hat{h}_{2,L}^*}{C_L}\right)-\hat{C}_1^*\frac{2\hat{h}_{2,L}}{C_L},$$

$$B_0\frac{1-2\nu_I}{2\mu_I(1-\nu_I)}+C_0r_0^2\frac{2\nu_I}{\mu_I(1-\nu_I)}=B_1\frac{1-2\nu_L}{2\mu_L(1-\nu_L)}+C_1r_0^2\frac{2\nu_L}{\mu_L(1-\nu_L)}+\frac{\hat{B}_1r_0^{-2}}{\mu_L}-$$
$$-\hat{C}_1r_0^{-4}\frac{3-2\nu_L}{\mu_L(1-\nu_L)}-A_1^*\frac{h_{2,L}^*}{C_L}-B_1^*\frac{h_{1,L}^*}{k_L}+C_1^*\frac{h_{2,L}}{C_L}-\hat{A}_1^*\frac{\hat{h}_{2,L}^*}{C_L}-\hat{B}_1^*\frac{\hat{h}_{1,L}^*}{k_L}+\hat{C}_1^*\frac{\hat{h}_{2,L}}{C_L},$$

$$A_0\frac{1-2\nu_I}{2\mu_I(1-\nu_I)}-C_0r_0^2\frac{2(3-2\nu_I)}{\mu_I(1-\nu_I)}=A_1\frac{1-2\nu_L}{2\mu_L(1-\nu_L)}-C_1r_0^2\frac{2(3-2\nu_L)}{\mu_L(1-\nu_L)}+$$
$$+\hat{A}_1r_0^{-2}\frac{1-2\nu_L}{2\mu_L(1-\nu_L)}-\hat{C}_1r_0^{-4}\frac{2(3-2\nu_L)}{\mu_L(1-\nu_L)}-A_1^*\frac{2h_{2,L}^*}{C_L}-C_1^*\left(\frac{h_{1,L}}{\mu_L}-\frac{2h_{2,L}}{C_L}\right)-$$
$$-\hat{A}_1^*\frac{2\hat{h}_{2,L}^*}{C_L}-\hat{C}_1^*\left(\frac{\hat{h}_{1,L}}{\mu_L}-\frac{2\hat{h}_{2,L}}{C_L}\right).$$

Equality of surface stresses at $r=r_0$, gives:

$$A_0\frac{1-2\nu_I}{1-\nu_I}=A_1\frac{1-2\nu_L}{1-\nu_L}-\frac{2\hat{A}_1r_0^{-2}}{1-\nu_L}-\hat{C}_1r_0^{-4}\frac{12(3-2\nu_L)}{1-\nu_L}+$$
$$+A_1^*\left(\frac{4\mu_L+\lambda_L}{k_L}h_{1,L}^*-\frac{2(6\mu_L+\lambda_L)}{C_L}h_{2,L}^*\right)-2C_1^*\left(h_{1,L}-\frac{6\mu_L+\lambda_L}{C_L}h_{2,L}\right)+$$
$$+\hat{A}_1^*\left(\frac{4\mu_L+\lambda_L}{k_L}\hat{h}_{1,L}^*-\frac{2(6\mu_L+\lambda_L)}{C_L}\hat{h}_{2,L}^*\right)-2\hat{C}_1^*\left(\hat{h}_{1,L}-\frac{6\mu_L+\lambda_L}{C_L}\hat{h}_{2,L}\right),$$

$$A_0\frac{\nu_I}{1-\nu_I}+\frac{B_0}{1-\nu_I}=A_1\frac{\nu_L}{1-\nu_L}+\frac{B_1}{1-\nu_L}+\hat{A}_1r_0^{-2}\frac{\nu_L}{1-\nu_L}-2\hat{B}_1r_0^{-2}+\hat{C}_1r_0^{-4}\frac{6(3-2\nu_L)}{1-\nu_L}+$$
$$+A_1^*\frac{6\mu_L+\lambda_L}{C_L}h_{2,L}^*+B_1^*\frac{4\mu_L+\lambda_L}{k_L}h_{1,L}^*+C_1^*\left(h_{1,L}-\frac{6\mu_L+\lambda_L}{C_L}h_{2,L}\right)+$$
$$+\hat{A}_1^*\frac{6\mu_L+\lambda_L}{C_L}\hat{h}_{2,L}^*+\hat{B}_1^*\frac{4\mu_L+\lambda_L}{k_L}\hat{h}_{1,L}^*-\hat{C}_1^*\left(\hat{h}_{1,L}-\frac{6\mu_L+\lambda_L}{C_L}\hat{h}_{2,L}\right),$$

$$A_0\frac{1-2\nu_I}{1-\nu_I}-C_0r_0^2\frac{12}{1-\nu_I}=A_1\frac{1-2\nu_L}{1-\nu_L}-C_1r_0^2\frac{12}{1-\nu_L}+\frac{\hat{A}_1r_0^{-2}}{1-\nu_L}+\hat{C}_1r_0^{-4}\frac{12(3-2\nu_L)}{1-\nu_L}+$$
$$+2A_1^*\left(\frac{\lambda_L}{k_L}h_{1,L}^*+\frac{3\mu_L-2\lambda_L}{C_L}h_{2,L}^*\right)+C_1^*\left(3h_{1,L}-\frac{2(3\mu_L-2\lambda_L)}{C_L}h_{2,L}\right)+$$
$$+2\hat{A}_1^*\left(\frac{\lambda_L}{k_L}\hat{h}_{1,L}^*+\frac{3\mu_L-2\lambda_L}{C_L}\hat{h}_{2,L}^*\right)+\hat{C}_1^*\left(3\hat{h}_{1,L}-\frac{2(3\mu_L-2\lambda_L)}{C_L}\hat{h}_{2,L}\right).$$

Equating the normal derivatives of displacements to zero, when $r=r_0$, gives:

$$A_1\frac{1-2\nu_L}{2\mu_L(1-\nu_L)}-C_1r_0^2\frac{12\nu_L}{\mu_L(1-\nu_L)}-\frac{\hat{A}_1r_0^{-2}}{\mu_L}-\hat{C}_1r_0^{-4}\frac{6(3-2\nu_L)}{\mu_L(1-\nu_L)}-2C_1^*\left(\frac{h_{1,L}}{\mu_L}-\frac{3h_{2,L}}{C_L}\right)+$$
$$+\frac{A_1^*}{k_L}\left(h_{1,L}^*-\left(r_0^2+\frac{6k_L}{C_L}\right)h_{2,L}^*\right)+\frac{\hat{A}_1^*}{k_L}\left(\hat{h}_{1,L}^*-\left(r_0^2+\frac{6k_L}{C_L}\right)\hat{h}_{2,L}^*\right)-2\hat{C}_1^*\left(\frac{\hat{h}_{1,L}}{\mu_L}-\frac{3\hat{h}_{2,L}}{C_L}\right)=0,$$

$$B_1\frac{1-2\nu_L}{2\mu_L(1-\nu_L)}+C_1r_0^2\frac{6\nu_L}{\mu_L(1-\nu_L)}-\frac{\hat{B}_1r_0^{-2}}{\mu_L}+\hat{C}_1r_0^{-4}\frac{3(3-2\nu_L)}{\mu_L(1-\nu_L)}-$$
$$-A_1^*\left(\frac{h_{1,L}^*}{k_L}-\frac{3h_{2,L}^*}{C_L}\right)-B_1^*\frac{h_{1,L}^*+r_0^2h_{2,L}^*}{k_L}+C_1^*\left(\frac{h_{1,L}}{\mu_L}-\frac{3h_{2,L}}{C_L}\right)-$$
$$-\hat{A}_1^*\left(\frac{\hat{h}_{1,L}^*}{k_L}-\frac{3\hat{h}_{2,L}^*}{C_L}\right)-\hat{B}_1^*\frac{\hat{h}_{1,L}^*+r_0^2\hat{h}_{2,L}^*}{k_L}+\hat{C}_1^*\left(\frac{\hat{h}_{1,L}}{\mu_L}-\frac{3\hat{h}_{2,L}}{C_L}\right)=0,$$

$$A_1\frac{1-2\nu_L}{2\mu_L(1-\nu_L)}-C_1r_0^2\frac{6(3-2\nu_L)}{\mu_L(1-\nu_L)}-\hat{A}_1r_0^{-2}\frac{1-2\nu_L}{2\mu_L(1-\nu_L)}+\hat{C}_1r_0^{-4}\frac{6(3-2\nu_L)}{\mu_L(1-\nu_L)}-$$
$$-2A_1^*\left(\frac{h_{1,L}^*}{k_L}-\frac{3h_{2,L}^*}{C_L}\right)+\frac{C_1^*}{\mu_L}\left(h_{1,L}-\left(r_0^2+\frac{6\mu_L}{C_L}\right)h_{2,L}\right)-$$
$$-2\hat{A}_1^*\left(\frac{\hat{h}_{1,L}^*}{k_L}-\frac{3\hat{h}_{2,L}^*}{C_L}\right)+\frac{\hat{C}_1^*}{\mu_L}\left(\hat{h}_{1,L}-\left(r_0^2+\frac{6\mu_L}{C_L}\right)\hat{h}_{2,L}\right)=0.$$

Equality of the displacements on the second boundary $r=r_1$ gives:

$$A_1\frac{1-2\nu_L}{2\mu_L(1-\nu_L)}-C_1r_1^2\frac{4\nu_L}{\mu_L(1-\nu_L)}+\frac{\hat{A}_1r_1^{-2}}{\mu_L}+\hat{C}_1r_1^{-4}\frac{2(3-2\nu_L)}{\mu_L(1-\nu_L)}-$$
$$-A_1^*\left(\frac{h_{1,L}^*}{k_L}-\frac{2h_{2,L}^*}{C_L}\right)-C_1^*\frac{2h_{2,L}}{C_L}-\hat{A}_1^*\left(\frac{\hat{h}_{1,L}^*}{k_L}-\frac{2\hat{h}_{2,L}^*}{C_L}\right)-\hat{C}_1^*\frac{2\hat{h}_{2,L}}{C_L}=$$
$$=A_2\frac{1-2\nu_M}{2\mu_M(1-\nu_M)}-C_2r_1^2\frac{4\nu_M}{\mu_M(1-\nu_M)}+\frac{\hat{A}_2r_1^{-2}}{\mu_M}+\hat{C}_2r_1^{-4}\frac{2(3-2\nu_M)}{\mu_M(1-\nu_M)},$$

$$B_1\frac{1-2\nu_L}{2\mu_L(1-\nu_L)}+C_1r_1^2\frac{2\nu_L}{\mu_L(1-\nu_L)}+\frac{\hat{B}_1r_1^{-2}}{\mu_L}-\hat{C}_1r_1^{-4}\frac{3-2\nu_L}{\mu_L(1-\nu_L)}-$$
$$-A_1^*\frac{h_{2,L}^*}{C_L}-B_1^*\frac{h_{1,L}^*}{k_L}+C_1^*\frac{h_{2,L}}{C_L}-\hat{A}_1^*\frac{\hat{h}_{2,L}^*}{C_L}-\hat{B}_1^*\frac{\hat{h}_{1,L}^*}{k_L}+\hat{C}_1^*\frac{\hat{h}_{2,L}}{C_L}=$$
$$=B_2\frac{1-2\nu_M}{2\mu_M(1-\nu_M)}+C_2r_1^2\frac{2\nu_M}{\mu_M(1-\nu_M)}+\frac{\hat{B}_2r_1^{-2}}{\mu_M}-\hat{C}_2r_1^{-4}\frac{3-2\nu_M}{\mu_M(1-\nu_M)},$$

$$A_1\frac{1-2\nu_L}{2\mu_L(1-\nu_L)}-C_1r_1^2\frac{2(3-2\nu_L)}{\mu_L(1-\nu_L)}+\hat{A}_1r_1^{-2}\frac{1-2\nu_L}{2\mu_L(1-\nu_L)}-\hat{C}_1r_1^{-4}\frac{2(3-2\nu_L)}{\mu_L(1-\nu_L)}-$$
$$-A_1^*\frac{2h_{2,L}^*}{C_L}-C_1^*\left(\frac{h_{1,L}}{\mu_L}-\frac{2h_{2,L}}{C_L}\right)-\hat{A}_1^*\frac{2\hat{h}_{2,L}^*}{C_L}-\hat{C}_1^*\left(\frac{\hat{h}_{1,L}}{\mu_L}-\frac{2\hat{h}_{2,L}}{C_L}\right)=$$
$$=A_2\frac{1-2\nu_M}{2\mu_M(1-\nu_M)}-C_2r_1^2\frac{2(3-2\nu_M)}{\mu_M(1-\nu_M)}+\hat{A}_2r_1^{-2}\frac{1-2\nu_M}{2\mu_M(1-\nu_M)}-\hat{C}_2r_1^{-4}\frac{2(3-2\nu_M)}{\mu_M(1-\nu_M)}.$$

Equality of surface stresses at the second boundary $r=r_1$ gives:

$$A_1\frac{1-2\nu_L}{1-\nu_L}-\frac{2\hat{A}_1 r_1^{-2}}{1-\nu_L}-\hat{C}_1 r_1^{-4}\frac{12(3-2\nu_L)}{1-\nu_L}+A_1^*\left(\frac{4\mu_L+\lambda_L}{k_L}h_{1,L}^*-\frac{2(6\mu_L+\lambda_L)}{C_L}h_{2,L}^*\right)-$$
$$-2C_1^*\left(h_{1,L}-\frac{6\mu_L+\lambda_L}{C_L}h_{2,L}\right)+\hat{A}_1^*\left(\frac{4\mu_L+\lambda_L}{k_L}\hat{h}_{1,L}^*-\frac{2(6\mu_L+\lambda_L)}{C_L}\hat{h}_{2,L}^*\right)-$$
$$-2\hat{C}_1^*\left(\hat{h}_{1,L}-\frac{6\mu_L+\lambda_L}{C_L}\hat{h}_{2,L}\right)=A_2\frac{1-2\nu_M}{1-\nu_M}-\frac{2\hat{A}_2 r_1^{-2}}{1-\nu_M}-\hat{C}_2 r_1^{-4}\frac{12(3-2\nu_M)}{1-\nu_M},$$

$$A_1\frac{\nu_L}{1-\nu_L}+\frac{B_1}{1-\nu_L}+\hat{A}_1 r_1^{-2}\frac{\nu_L}{1-\nu_L}-2\hat{B}_1 r_1^{-2}+\hat{C}_1 r_1^{-4}\frac{6(3-2\nu_L)}{1-\nu_L}+$$
$$+A_1^*\frac{6\mu_L+\lambda_L}{C_L}h_{2,L}^*+B_1^*\frac{4\mu_L+\lambda_L}{k_L}h_{1,L}^*+C_1^*\left(h_{1,L}-\frac{6\mu_L+\lambda_L}{C_L}h_{2,L}\right)+$$
$$+\hat{A}_1^*\frac{6\mu_L+\lambda_L}{C_L}\hat{h}_{2,L}^*+\hat{B}_1^*\frac{4\mu_L+\lambda_L}{k_L}\hat{h}_{1,L}^*+\hat{C}_1^* r_1^{-2}\left(\hat{h}_{1,L}-\frac{6\mu_L+\lambda_L}{C_L}\hat{h}_{2,L}\right)=$$
$$=A_2\frac{\nu_M}{1-\nu_M}+\frac{B_2}{1-\nu_M}+\hat{A}_2 r_1^{-2}\frac{\nu_M}{1-\nu_M}-2\hat{B}_2 r_1^{-2}+\hat{C}_2 r_1^{-4}\frac{6(3-2\nu_M)}{1-\nu_M},$$

$$A_1\frac{1-2\nu_L}{1-\nu_L}-C_1 r_1^2\frac{12}{1-\nu_L}+\frac{\hat{A}_1 r_1^{-2}}{1-\nu_L}+\hat{C}_1 r_1^{-4}\frac{12(3-2\nu_L)}{1-\nu_L}+$$
$$+2A_1^*\left(\frac{\lambda_L}{k_L}h_{1,L}^*+\frac{3\mu_L-2\lambda_L}{C_L}h_{2,L}^*\right)+C_1^*\left(3h_{1,L}-\frac{2(3\mu_L-2\lambda_L)}{C_L}h_{2,L}\right)+$$
$$+2\hat{A}_1^*\left(\frac{\lambda_L}{k_L}\hat{h}_{1,L}^*+\frac{3\mu_L-2\lambda_L}{C_L}\hat{h}_{2,L}^*\right)+\hat{C}_1^*\left(3\hat{h}_{1,L}-\frac{2(3\mu_L-2\lambda_L)}{C_L}\hat{h}_{2,L}\right)=$$
$$=A_2\frac{1-2\nu_M}{1-\nu_M}-C_2 r_1^2\frac{12}{1-\nu_M}+\frac{\hat{A}_2 r_1^{-2}}{1-\nu_M}+\hat{C}_2 r_1^{-4}\frac{12(3-2\nu_M)}{1-\nu_M}.$$

Equating the normal derivatives of displacements to zero at the second boundary $r=r_1$ gives:

$$A_1\frac{1-2\nu_L}{2\mu_L(1-\nu_L)}-C_1 r_1^2\frac{12\nu_L}{\mu_L(1-\nu_L)}-\frac{\hat{A}_1 r_1^{-2}}{\mu_L}-\hat{C}_1 r_0^{-4}\frac{6(3-2\nu_L)}{\mu_L(1-\nu_L)}-2C_1^*\left(\frac{h_{1,L}}{\mu_L}-\frac{3h_{2,L}}{C_L}\right)+$$
$$+\frac{A_1^*}{k_L}\left(h_{1,L}^*-\left(r_1^2+\frac{6k_L}{C_L}\right)h_{2,L}^*\right)+\frac{\hat{A}_1^*}{k_L}\left(\hat{h}_{1,L}^*-\left(r_1^2+\frac{6k_L}{C_L}\right)\hat{h}_{2,L}^*\right)-2\hat{C}_1^*\left(\frac{\hat{h}_{1,L}}{\mu_L}-\frac{3\hat{h}_{2,L}}{C_L}\right)=0,$$

$$B_1\frac{1-2\nu_L}{2\mu_L(1-\nu_L)}+C_1 r_1^2\frac{6\nu_L}{\mu_L(1-\nu_L)}-\frac{\hat{B}_1 r_1^{-2}}{\mu_L}+\hat{C}_1 r_1^{-4}\frac{3(3-2\nu_L)}{\mu_L(1-\nu_L)}-$$
$$-A_1^*\left(\frac{h_{1,L}^*}{k_L}-\frac{3h_{2,L}^*}{C_L}\right)-B_1^*\frac{h_{1,L}^*+r_1^2 h_{2,L}^*}{k_L}+C_1^*\left(\frac{h_{1,L}}{\mu_L}-\frac{3h_{2,L}}{C_L}\right)-$$
$$-\hat{A}_1^*\left(\frac{\hat{h}_{1,L}^*}{k_L}-\frac{3\hat{h}_{2,L}^*}{C_L}\right)-\hat{B}_1^*\frac{\hat{h}_{1,L}^*+r_1^2\hat{h}_{2,L}^*}{k_L}+\hat{C}_1^*\left(\frac{\hat{h}_{1,L}}{\mu_L}-\frac{3\hat{h}_{2,L}}{C_L}\right)=0,$$

$$A_1\frac{1-2\nu_L}{2\mu_L(1-\nu_L)}-C_1r_1^2\frac{6(3-2\nu_L)}{\mu_L(1-\nu_L)}-\hat{A}_1r_1^{-2}\frac{1-2\nu_L}{2\mu_L(1-\nu_L)}+\hat{C}_1r_1^{-4}\frac{6(3-2\nu_L)}{\mu_L(1-\nu_L)}-$$
$$-2A_1^*\left(\frac{h_{1,L}^*}{k_L}-\frac{3h_{2,L}^*}{C_L}\right)+\frac{C_1^*}{\mu_L}\left(h_{1,L}-\left(r_1^2+\frac{6\mu_L}{C_L}\right)h_{2,L}\right)-$$
$$-2\hat{A}_1^*\left(\frac{\hat{h}_{1,L}^*}{k_L}-\frac{3\hat{h}_{2,L}^*}{C_L}\right)+\frac{\hat{C}_1^*}{\mu_L}\left(\hat{h}_{1,L}-\left(r_1^2+\frac{6\mu_L}{C_L}\right)\hat{h}_{2,L}\right)=0.$$

Finally, two contact conditions on the boundary of the region G_H are derived by equating displacements and surface forces at the external boundary $r=r_2$. Equality of displacements gives:

$$A_2\frac{1-2\nu_M}{2\mu_M(1-\nu_M)}-C_2r_2^2\frac{4\nu_M}{\mu_M(1-\nu_M)}+\frac{\hat{A}_2r_2^{-2}}{\mu_M}+\hat{C}_2r_2^{-4}\frac{2(3-2\nu_M)}{\mu_M(1-\nu_M)}=$$
$$=\frac{1-2\nu_H}{2\mu_H(1-\nu_H)}+\frac{\hat{A}_3r_2^{-2}}{\mu_H}+\hat{C}_3r_2^{-4}\frac{2(3-2\nu_H)}{\mu_H(1-\nu_H)},$$
$$B_2\frac{1-2\nu_M}{2\mu_M(1-\nu_M)}+C_2r_2^2\frac{2\nu_M}{\mu_M(1-\nu_M)}+\frac{\hat{B}_2r_2^{-2}}{\mu_M}-\hat{C}_2r_2^{-4}\frac{3-2\nu_M}{\mu_M(1-\nu_M)}=$$
$$=\frac{1-2\nu_H}{2\mu_H(1-\nu_H)}+\frac{\hat{B}_3r_2^{-2}}{\mu_H}-\hat{C}_3r_2^{-4}\frac{3-2\nu_H}{\mu_H(1-\nu_H)},$$
$$A_2\frac{1-2\nu_M}{2\mu_M(1-\nu_M)}-C_2r_2^2\frac{2(3-2\nu_M)}{\mu_M(1-\nu_M)}+\hat{A}_2r_2^{-2}\frac{1-2\nu_M}{2\mu_M(1-\nu_M)}-\hat{C}_2r_2^{-4}\frac{2(3-2\nu_M)}{\mu_M(1-\nu_M)}=$$
$$=\frac{1-2\nu_H}{2\mu_H(1-\nu_H)}+\hat{A}_3r_2^{-2}\frac{1-2\nu_H}{2\mu_H(1-\nu_H)}-\hat{C}_3r_2^{-4}\frac{2(3-2\nu_H)}{\mu_H(1-\nu_H)}.$$

Equality of surface forces at $r=r_2$ gives:

$$A_2\frac{1-2\nu_M}{1-\nu_M}-\frac{2\hat{A}_2r_2^{-2}}{1-\nu_M}-\hat{C}_2r_2^{-4}\frac{12(3-2\nu_M)}{1-\nu_M}=\frac{1-2\nu_H}{1-\nu_H}-\frac{2\hat{A}_3r_2^{-2}}{1-\nu_H}-\hat{C}_3r_2^{-4}\frac{12(3-2\nu_H)}{1-\nu_H},$$
$$A_2\frac{\nu_M}{1-\nu_M}+\frac{B_2}{1-\nu_M}+\hat{A}_2r_2^{-2}\frac{\nu_M}{1-\nu_M}-2\hat{B}_2r_2^{-2}+\hat{C}_2r_2^{-4}\frac{6(3-2\nu_M)}{1-\nu_M}=$$
$$=\frac{\nu_H}{1-\nu_H}+\hat{A}_3r_2^{-2}\frac{\nu_H}{1-\nu_H}-2\hat{B}_3r_2^{-2}+\hat{C}_3r_2^{-4}\frac{6(3-2\nu_H)}{1-\nu_H},$$
$$A_2\frac{1-2\nu_M}{1-\nu_M}-C_2r_2^2\frac{12}{1-\nu_M}+\frac{\hat{A}_2r_2^{-2}}{1-\nu_M}+\hat{C}_2r_2^{-4}\frac{12(3-2\nu_M)}{1-\nu_M}=$$
$$=\frac{1-2\nu_H}{1-\nu_H}+\frac{\hat{A}_3r_2^{-2}}{1-\nu_H}+\hat{C}_3r_2^{-4}\frac{12(3-2\nu_H)}{1-\nu_H}.$$

As a result, we obtain 24 equations for the 24 unknown coefficients A_0, B_0, C_0, A_1, B_1, C_1, $\hat{A}_1$, $\hat{B}_1$, $\hat{C}_1$, A_1^*, B_1^*, C_1^*, $\hat{A}_1^*$, $\hat{B}_1^*$, $\hat{C}_1^*$, A_2, B_2, C_2, $\hat{A}_2$, $\hat{B}_2$, $\hat{C}_2$, $\hat{A}_3$, $\hat{B}_3$, $\hat{C}_3$. By the solving of them we obtain the solution of the generalized Eshelby problem in the form of Papkovich-Neuber representations for the potentials given by Eqs. (22) – (24) for any homogeneous state of deformation at infinity, defined by arbitrary harmonic polynomials of first order.